
Learning Spatiotemporal Sensitivity in Video LLMs via Counterfactual Reinforcement Learning

Dazhao Du^{1,2*} Jian Liu¹ Jialong Qin¹ Tao Han¹ Bohai Gu¹
 Fangqi Zhu¹ Yujia Zhang² Eric Liu² Xi Chen² Song Guo^{1†}

¹Hong Kong University of Science and Technology ²Tencent

Abstract

Video large language models (Video LLMs) achieve strong benchmark accuracy, yet often answer video questions through shortcuts such as single-frame cues and language priors rather than by tracking spatiotemporal dynamics. This issue is exacerbated in RL post-training, where correctness-only rewards can further reinforce shortcut policies that obtain high reward without tracking video dynamics. We address this by asking a controlled counterfactual question: if the visual world changed while the question remained fixed, should the answer change or stay the same? Based on this view, we propose **Counterfactual Relational Policy Optimization (CRPO)**, a dual-branch RL framework for improving *spatiotemporal sensitivity*. CRPO constructs counterfactual videos through horizontal flips and temporal reversals, trains on both original and counterfactual branches, and introduces a **Counterfactual Relation Reward (CRR)** between their answers. CRR encourages answers to change for dynamic questions and remain unchanged for static questions. This cross-branch constraint makes it difficult for shortcut policies to be consistently rewarded across both branches. To evaluate this property, we introduce **DyBench**, a paired counterfactual video benchmark with 3,014 videos covering reversible dynamics, moving direction, and event sequence, together with a strict pair-accuracy metric that prevents fixed-answer shortcuts from inflating scores. Experiments show that CRPO outperforms prior RL methods on spatiotemporal-sensitive evaluations while maintaining competitive general video performance. On Qwen3-VL-8B, CRPO improves DyBench P-Acc by +7.7 and TimeBlind I-Acc by +8.2 over the base model, indicating improved spatiotemporal sensitivity rather than stronger reliance on static shortcuts. The project website can be found at <https://ddz16.github.io/crpo.github.io/>.

1 Introduction

Video large language models (Video LLMs) [51, 2, 42, 32] have achieved strong results on video understanding benchmarks [11, 24]. Yet recent studies [20, 54, 21, 18] suggest that high accuracy does not necessarily reflect genuine spatiotemporal understanding. Models can often answer correctly by exploiting static shortcuts, such as single-frame cues and language priors, rather than tracking how events unfold over time. Figure 1 illustrates this failure: Qwen3-VL [2] answers a static object-presence question correctly, but fails on movement direction and gives the same prediction to a video and its temporal reversal. Across MVBench [24] and TempCompass [29], accuracy also drops as the

*Part of this work was done while Dazhao was an intern at Tencent.

†Corresponding author.

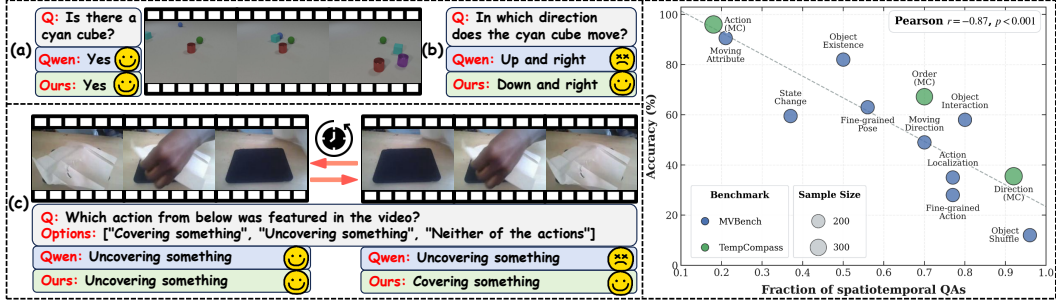


Figure 1: **Current Video LLMs remain insensitive to spatiotemporal changes.** **Left:** On the same scene, the model (a) answers a static question correctly, but (b) fails on a spatiotemporal question; (c) it gives the same prediction to a video and its temporal reversal. **Right:** Across MV-Bench and TempCompass sub-tasks, accuracy drops as the fraction of spatiotemporal questions increases.

fraction of spatiotemporal questions increases, with direction, fine-grained action, and object-shuffle tasks among the hardest. These patterns suggest that current Video LLMs often recognize what is visible, but remain insensitive to how visual states change.

This shortcut problem becomes especially consequential in reinforcement learning. RL post-training has recently become a powerful recipe for LLMs [13, 48] and Video LLMs [9, 40, 25], but GRPO-style RL typically relies on correctness-only rewards that evaluate the final answer alone. If a single frame or a language-based guess is enough to answer a training question, the policy can receive high reward without tracking video dynamics. In this way, correctness-only RL may reinforce shortcut policies: it improves benchmark accuracy without ensuring that the answer is grounded in the video’s spatiotemporal content, and can even weaken the model’s sensitivity to dynamic evidence [47].

A direct solution would be to reward the model for using explicit spatiotemporal evidence in its reasoning process [49, 34]. However, this requires constructing or annotating high-quality evidence traces, which is expensive and difficult to scale. We instead ask whether shortcut reliance can be reduced with a much simpler signal. Our observation is that a model should respond predictably to controlled counterfactual visual worlds: the question remains fixed, while the spatiotemporal evidence is altered to ask what the answer would have been under the changed visual condition. If an object moving right is horizontally flipped or temporally reversed, a spatiotemporally sensitive model should change its answer; if the question asks about a static attribute such as object presence or color, the answer should remain unchanged. We call this property *spatiotemporal sensitivity*: equivariance for dynamic questions and invariance for static questions. Such a behavioral signature is difficult for static shortcut policies to satisfy consistently.

Based on this principle, we propose **Counterfactual Relational Policy Optimization (CRPO)**, a simple dual-branch extension of GRPO that rewards the *relation* between answers to factual and counterfactual videos. For each training prompt, a **Task Router** selects a controlled transformation, such as horizontal flip or temporal reversal, according to whether the question is spatial, temporal, spatiotemporal, or static. CRPO then samples rollouts from both the factual video and its counterfactual visual counterpart. Its **Counterfactual Relation Reward (CRR)** rewards whether the answer relation across the two branches matches the expected effect of the visual change: answer changes for dynamic questions and answer agreement for static questions, without requiring counterfactual ground-truth labels or spatiotemporal annotations. Unlike prior video RL methods [9, 45] that use a perturbed video only to shape rewards on the original branch, CRPO updates the policy from both branches. Thus, the counterfactual branch is not merely a passive diagnostic signal, but directly contributes policy gradients that train the model to become sensitive to task-relevant visual changes.

To evaluate this property directly, we further introduce **DyBench**, a paired counterfactual benchmark with 3,014 videos spanning three sub-tasks: reversible dynamics, moving direction, and event sequence. Each pair contains an original video and its counterfactual counterpart, sharing the same question but requiring different answers. We report *pair accuracy* (P-Acc), which counts a pair as correct only when both videos are answered correctly, preventing fixed-answer shortcut policies from inflating scores. Experiments on Qwen3-VL show that CRPO consistently improves spatiotemporal-sensitive benchmarks while preserving general video understanding.

Our main contributions are:

- We propose **Counterfactual Relational Policy Optimization (CRPO)**, a simple dual-branch RL framework for improving *spatiotemporal sensitivity* in Video LLMs. CRPO trains on both original and counterfactual branches and uses a **Counterfactual Relation Reward (CRR)** to reward equivariant or invariant answer relations, discouraging shortcut reliance without requiring counterfactual labels or costly spatiotemporal evidence annotations.
- We introduce **DyBench**, a 3,014-video paired counterfactual benchmark with strict pair accuracy, and show that CRPO improves spatiotemporal-sensitive evaluations such as DyBench and TimeBlind while maintaining competitive general video performance.

2 Related Works

Video Large Language Models. The rapid progress of large language models [32, 36] has driven substantial advances in video understanding. Recent Video LLMs typically extend the image-language instruction-tuning paradigm [27] to video by bridging video and text modalities through lightweight adapters or projectors, and by training on large-scale video-caption and video instruction-following data [22, 50, 51]. More recent open models [5, 6, 42, 2] further strengthen multimodal reasoning, grounding, and long-context modeling through better data and training pipelines. Some work improves long-video understanding through memory, compression, or token reduction [37, 35, 33]. Despite these advances, strong benchmark performance does not necessarily imply genuine spatiotemporal understanding, as many Video LLMs can still rely on static shortcuts such as single-frame cues or language priors [54, 18] rather than truly modeling how events unfold over time.

RL for Video LLMs. Recent work has explored reinforcement learning for Video LLMs. GRPO [13] has become a common foundation for RL-based post-training, motivating studies on data selection, reward design, optimization stability, and credit assignment [25, 40, 31, 10, 28, 44]. These works show that video RL depends critically on how reward signals are designed. Several recent methods further introduce video variations into RL. Video-R1 [9] (T-GRPO) shuffles frames and rewards original-video rollouts when they outperform shuffled-video rollouts, while ArrowRL [45] uses temporal reversal to penalize original-video rollouts that mirror reversed-video responses. These perturbations provide useful contrastive signals, but the perturbed videos are used only for reward shaping. STRIVE [1] groups rollouts jointly over textual outputs and spatiotemporal visual variants to improve exploration. CRPO follows the direction of using video variations, but treats the counterfactual video as a trainable branch: both original and counterfactual branches generate rollouts and contribute policy gradients. The Counterfactual Relation Reward then links the two branches by rewarding answer changes for dynamic questions and answer preservation for static questions, yielding a simple and targeted signal for spatiotemporal sensitivity.

Video Understanding Benchmarks. Standard benchmarks [11, 24, 41, 52] cover broad video understanding abilities, but they do not explicitly diagnose shortcut-based success. Recent diagnostic benchmarks aim to close this gap. TempCompass [29] probes temporal perception with conflicting videos matched in static content. MHBench [17] uses adversarial triplets to evaluate motion hallucination and test whether Video LLMs rely on static appearance instead of true motion perception. MVP [18] uses minimal-change video pairs with identical questions and opposite answers to reduce shortcut-based score inflation. TimeBlind [21] is closest to our setting, using minimal video pairs and paired evaluation to isolate temporal understanding. Our proposed *DyBench* follows this line, but frames paired evaluation through counterfactual video pairs. It focuses on three spatiotemporal tasks, namely reversible dynamics, moving direction, and event sequence, and uses *pair accuracy* to distinguish shortcut success from genuine spatiotemporal understanding.

3 Counterfactual Relational Policy Optimization

Standard GRPO [13] rewards answer correctness alone, so a policy that exploits single-frame cues or language priors can obtain high reward without genuinely understanding spatiotemporal dynamics. This can reinforce shortcut policies rather than improve spatiotemporal sensitivity. We instead evaluate a model through a controlled counterfactual question: if the visual world changes while the question remains fixed, should the answer change or stay the same? This yields two desired behaviors:

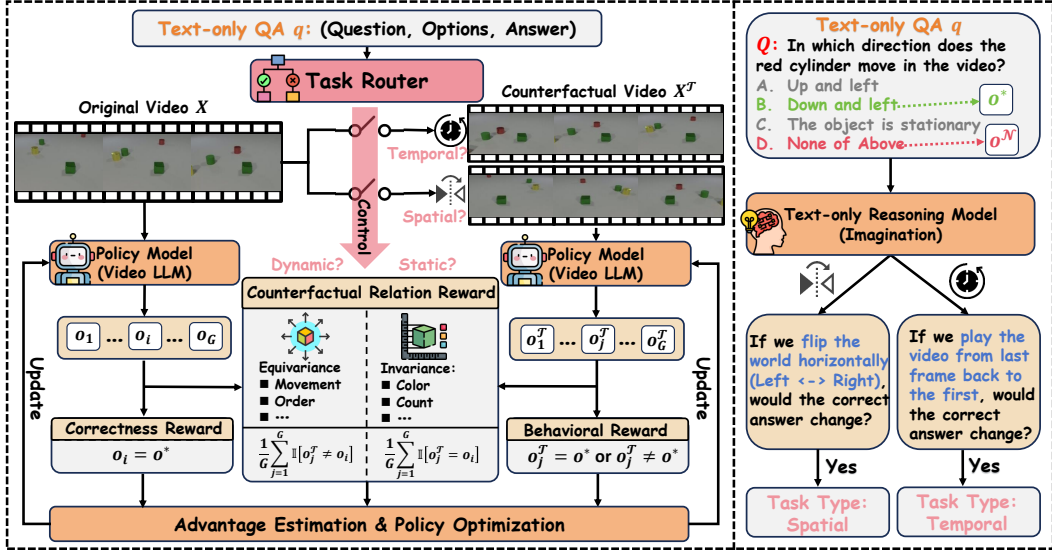


Figure 2: **Overview of CRPO.** **Left:** Given a video question, the Task Router selects a counterfactual transformation \mathcal{T} (horizontal flip or temporal reversal). The original branch and the counterfactual branch each generate G rollouts. These rollouts are scored by branch-specific correctness or behavioral rewards, format rewards, and the Counterfactual Relation Reward (CRR), and are then used for advantage estimation and policy optimization. **Right:** The Task Router is implemented as a text-only reasoning model that answers two hypothetical transformation questions to predict whether the correct answer would change under horizontal flip or temporal reversal.

equivariance, changing the answer when task-relevant dynamics are perturbed, and *invariance*, preserving the answer when the question concerns a static attribute unaffected by the perturbation.

CRPO operationalizes this counterfactual view as a dual-branch extension of GRPO. As illustrated in the left panel of Figure 2, given a video X and question Q , a **Task Router** classifies Q into one of four task types and selects the corresponding transformation \mathcal{T} . The *original branch* feeds (X, Q) to the policy and generates a group of G rollouts $\{o_1, \dots, o_G\}$, while the *counterfactual branch* applies \mathcal{T} to produce $X^{\mathcal{T}}$ and generates a parallel group $\{o_1^{\mathcal{T}}, \dots, o_G^{\mathcal{T}}\}$ from $(X^{\mathcal{T}}, Q)$. The **Counterfactual Relation Reward (CRR)** then rewards the policy when the answers across the two groups match the expected behavior for the question’s task type, namely answer changes for dynamic questions and answer agreement for static questions, a cross-branch relation that is difficult for single-frame or language shortcuts to satisfy consistently.

Task Router. Different questions require different counterfactual transformations. A spatial question about direction calls for a horizontal flip, while a temporal question about event ordering calls for temporal reversal. To determine the appropriate transformation, we define a task-type function $\mathcal{T}(q)$ that maps each question–options–answer tuple q to one of four categories, Spatial, Temporal, Spatiotemporal, or Static.

As shown in the right panel of Figure 2, we classify task types using a text-only reasoning model that receives only the question, answer options, and ground-truth answer, without any visual input. The model answers two hypothetical questions via *imagination*, (1) “If we flip the world horizontally (Left \leftrightarrow Right), would the correct answer change?” and (2) “If we play the video from last frame back to the first, would the correct answer change?” The joint responses determine the task type. A *yes* to only the first question yields Spatial, a *yes* to only the second yields Temporal, a *yes* to both yields Spatiotemporal, and a *no* to both yields Static. This classification is performed *offline* before training, incurring no additional cost during reinforcement learning.

Once the task type is determined, the counterfactual transformation is applied accordingly. Spatial questions use horizontal flip, Temporal questions use temporal reversal, and Spatiotemporal questions randomly select one of the two with equal probability. For Static questions, the answer

is, by definition, invariant to both transformations, so we likewise sample uniformly between flip and reversal. Their reward signal then encourages answer invariance rather than change.

Counterfactual Relation Reward (CRR). Let $\{o_1, \dots, o_G\}$ and $\{o_1^T, \dots, o_G^T\}$ denote the rollout outputs from the original and counterfactual branches, respectively, and let o^* be the ground-truth answer. CRR assigns a reward to each rollout by combining a branch-specific base reward with a cross-branch relational term that measures whether the answer relation across branches matches the expected behavior for the given task type. We categorize `Spatial`, `Temporal`, and `Spatiotemporal` collectively as *dynamic* tasks, and `Static` as *static* tasks.

Original branch. The reward for the i -th original-branch rollout o_i is:

$$R_{\text{orig}}(o_i) = R_{\text{correct}}(o_i) + R_{\text{CRR}}^{\text{orig}}(o_i) + R_{\text{format}}(o_i), \quad (1)$$

where $R_{\text{correct}}(o_i) = \mathbb{I}[o_i = o^*]$ is the standard correctness reward and R_{format} penalizes malformed outputs. The cross-branch relational term $R_{\text{CRR}}^{\text{orig}}$ measures whether the counterfactual branch outputs behave as expected, gated on the original rollout being correct,

$$R_{\text{CRR}}^{\text{orig}}(o_i) = \mathbb{I}[o_i = o^*] \cdot \begin{cases} \frac{\lambda_d}{G} \sum_{j=1}^G \mathbb{I}[o_j^T \neq o_i], & \text{dynamic task,} \\ \frac{\lambda_s}{G} \sum_{j=1}^G \mathbb{I}[o_j^T = o_i], & \text{static task,} \end{cases} \quad (2)$$

where λ_d and λ_s are weighting coefficients for dynamic and static tasks, respectively. For dynamic tasks, $R_{\text{CRR}}^{\text{orig}}$ rewards equivariance by measuring the fraction of counterfactual rollouts whose answers differ from the original. For static tasks, it rewards invariance by measuring the fraction that agree.

Counterfactual branch. The reward for the j -th counterfactual-branch rollout o_j^T is:

$$R_{\text{aug}}(o_j^T) = w_{\text{aug}} \cdot (R_{\text{behave}}(o_j^T) + R_{\text{CRR}}^{\text{aug}}(o_j^T) + R_{\text{format}}(o_j^T)), \quad (3)$$

where w_{aug} controls the overall influence of the counterfactual branch relative to the original. The behavioral reward R_{behave} evaluates whether each counterfactual rollout exhibits the expected response to the transformation, *independently* of the original branch,

$$R_{\text{behave}}(o_j^T) = \begin{cases} \mathbb{I}[o_j^T \neq o^*], & \text{dynamic task,} \\ \mathbb{I}[o_j^T = o^*], & \text{static task.} \end{cases} \quad (4)$$

For dynamic tasks, the model is rewarded when its answer changes under the counterfactual input ($o_j^T \neq o^*$), and for static tasks when it remains correct ($o_j^T = o^*$). The relational term $R_{\text{CRR}}^{\text{aug}}$ measures whether the original branch also answers correctly, gated on the counterfactual rollout exhibiting the expected behavior,

$$R_{\text{CRR}}^{\text{aug}}(o_j^T) = R_{\text{behave}}(o_j^T) \cdot \frac{\lambda}{G} \sum_{k=1}^G \mathbb{I}[o_k = o^*], \quad (5)$$

where $\lambda = \lambda_d$ for dynamic tasks and $\lambda = \lambda_s$ for static tasks. This creates a symmetric mutual reward between the two branches. The original branch’s $R_{\text{CRR}}^{\text{orig}}$ checks whether counterfactual outputs change or stay as expected, while the counterfactual branch’s $R_{\text{CRR}}^{\text{aug}}$ checks whether original outputs are correct. The highest reward is therefore achieved when the original branch answers correctly and the counterfactual branch exhibits the expected behavior, i.e., changing its answer for dynamic tasks and preserving it for static tasks. For the counterfactual branch, CRR does not require an independent label. It uses the expected relation to the original branch as the reward signal.

Optimization. For each prompt, GRPO generates a group of G rollouts and computes per-rollout advantages by subtracting the group mean reward and normalizing by the group standard deviation. CRPO extends this to two branches. Inspired by the observation that per-group standard deviation can be unstable or uninformative in small rollout groups [15, 30], we adopt a hybrid normalization strategy: each branch’s rewards are centered by subtracting the branch-specific group mean (preserving the intra-group ranking), but the standard deviation is computed jointly over both branches’ centered

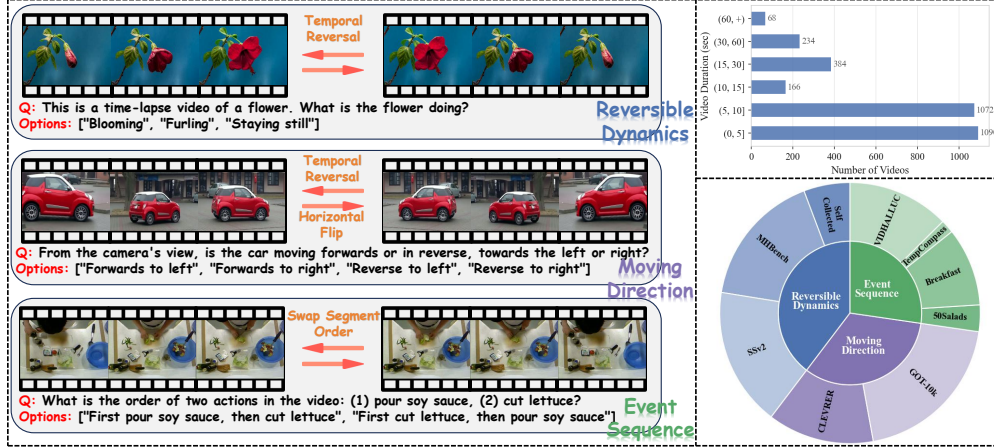


Figure 3: **Overview of DyBench.** 3,014 paired counterfactual videos across three sub-tasks: reversible dynamics, moving direction, and event sequence.

rewards ($2G$ values per prompt). This naturally places the two branches on a common scale (see Appendix F for a detailed analysis). Let \hat{A}_i and \hat{A}_j^T denote the normalized advantages for the original and counterfactual rollouts, and let ρ_i, ρ_j^T be the corresponding importance sampling ratios $\pi_\theta / \pi_{\theta_{\text{old}}}$. The per-prompt CRPO objective is:

$$\mathcal{L}_{\text{CRPO}}(\theta) = \underbrace{\frac{1}{G} \sum_{i=1}^G \min(\rho_i \hat{A}_i, \text{clip}(\rho_i, 1-\epsilon, 1+\epsilon) \hat{A}_i)}_{\text{original branch}} + \underbrace{\frac{1}{G} \sum_{j=1}^G \min(\rho_j^T \hat{A}_j^T, \text{clip}(\rho_j^T, 1-\epsilon, 1+\epsilon) \hat{A}_j^T)}_{\text{counterfactual branch}}. \quad (6)$$

The final loss averages Eq. 6 over all prompts in the batch, with a KL penalty omitted here for brevity. Both branches update the same policy π_θ , so the counterfactual branch directly shapes the model’s spatiotemporal sensitivity within the same GRPO-style optimization framework.

Null Option. After a counterfactual transformation such as temporal reversal, the correct answer for the transformed video may no longer appear among the original multiple-choice options. For example, if the original video shows an object moving left and down (option A) and the video is reversed, the correct answer becomes “moving right and up”, which may not be listed. To provide a valid output target in such cases, we append a *null option* σ^N (“None of the above”) to all multiple-choice questions. For the original branch, the ground-truth answer is always among the original options, so σ^N should not be selected. For the counterfactual branch on dynamic tasks, if the transformed correct answer is not among the original options, the model can select σ^N to express that the original answer is no longer valid. This counts as $\rho_j^T \neq \rho^*$ and triggers the equivariance reward via R_{behave} . For static tasks, the answer is unaffected by the transformation, so σ^N remains incorrect. This mechanism allows the counterfactual branch to express answer changes even when the transformed answer is not explicitly listed, without requiring counterfactual answer labels.

4 DyBench: A Paired Benchmark for Spatiotemporal Sensitivity

Existing video benchmarks are dominated by questions whose answers can be inferred from a single frame or a language prior [18, 21], leaving open the question of whether a Video LLM truly tracks spatiotemporal dynamics. To diagnose this directly, we construct **DyBench**, a paired counterfactual benchmark of 1,507 video pairs (3,014 videos) targeting motion direction, event order, and the arrow of time, the three aspects of a video that are most readily masked by static shortcuts.

Counterfactual pairs and pair accuracy. Each DyBench item is a *counterfactual pair* (v, v') rather than a single video. The two videos share the same scene and objects, ask the same multiple-choice question, and use the same option set; they differ only along a single spatiotemporal axis

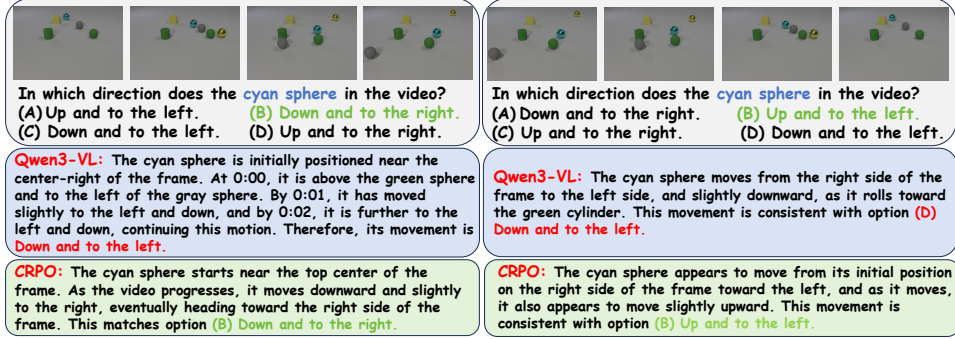


Figure 4: **Qualitative example.** For a temporally reversed video pair, the baseline Qwen3-VL predicts the same action label for both videos, whereas CRPO changes its answer and matches both ground truths. More examples are in Appendix G.

introduced by a controlled transformation, and consequently have *different* correct answers. We then report **pair accuracy** (P-Acc), which counts a pair as correct only when the model answers both v and v' correctly. By construction, P-Acc cannot be inflated by static-shortcut policies that always return the same answer for both sides of a pair: such policies score zero on every pair regardless of how confident their per-question answer is. The gap between P-Acc and the standard per-question accuracy (Acc) therefore indicates how much of a model’s accuracy reflects sensitivity to spatiotemporal changes rather than a fixed answer applied to both sides of the pair.

Three sub-tasks. A pair-construction transformation must (i) preserve the scene and objects, yet (ii) change the answer to a question about *spatiotemporal* content. Three transformations satisfy both: **temporal reversal** (play the clip backward), **horizontal flip** (mirror left–right), and **segment reordering** (swap the order of two action segments). These three transformations directly motivate the three DyBench sub-tasks. **(1) Reversible Dynamics** asks whether a change happens forward or backward in time (e.g., *opening vs. closing a door, a flower blooming vs. a flower closing*), built by playing clips forward and backward. **(2) Moving Direction** asks the direction in which an object or actor moves (e.g., *left vs. right*), built by horizontal flip and/or temporal reversal. **(3) Event Sequence** asks the order in which two events occur (e.g., *pour milk then pour cereals vs. pour cereals then pour milk*), built by concatenating two action segments in both orders. As shown in Figure 3, DyBench draws videos from a diverse set of sources covering humans, objects, animals, and plants, with most clips under 30 seconds. Further details are provided in Appendix A.

5 Experiments

5.1 Experimental Setup

Benchmarks. We evaluate on five benchmarks. DyBench (Sec. 4) and TimeBlind [21] are paired benchmarks for which we report both standard accuracy (Acc) and the strict paired metric, pair accuracy (P-Acc) for DyBench and instance accuracy (I-Acc) for TimeBlind. The other three, TempCompass [29], VideoMME [11], and MVBench [24], use standard accuracy alone. All evaluations are conducted with VLMEvalKit [8] at 32 uniformly sampled frames.

Baselines. We compare CRPO against two proprietary models (GPT-5.1 and Gemini-3.1-Pro), and four open-source backbones (LLaVA-OneVision-7B [22], InternVL3-8B [42], Qwen2.5-VL-7B [3], and ArrowRL*, the officially released checkpoint of [45]). Besides, we fairly compare our CRPO with other RL algorithms, including GRPO [13], T-GRPO [9], and ArrowRL [45]. All RL post-training methods share the same data, backbone, and training settings. More details are given in Appendix B.3.

Training Details. We instantiate CRPO on Qwen3-VL-4B-Instruct and Qwen3-VL-8B-Instruct [2], and follow the same training corpus and RL hyperparameters as VideoAuto-R1 [28]. The video subset contains 21,165 samples and is processed with $G=8$ rollouts per branch, 32 uniformly sampled frames per video, and a learning rate of 1×10^{-6} . The two CRPO-specific coefficients are set to $\lambda_d=\lambda_s=0.3$ and $w_{aug}=0.5$. The Task Router is run once offline using DeepSeek-R1, which agrees

Table 1: **Main results on five benchmarks.** Improvements of CRPO over the corresponding base model are marked with \uparrow .

Models	Spatiotemporal-Sensitive					General	
	DyBench		TimeBlind		TempCompass	VideoMME	MVBench
	Acc	P-Acc	Acc	I-Acc	Acc	Acc	Acc
<i>Proprietary Models</i>							
GPT-5.1 [36]	63.7	44.9	67.3	27.0	76.4	72.9	62.9
Gemini-3.1-Pro [32]	82.2	71.7	77.2	45.5	74.5	74.3	73.6
<i>Open-Source Models</i>							
LLaVA-OV-7B [22]	48.4	19.6	56.5	7.8	60.5	57.6	54.7
InternVL3-8B [42]	69.5	50.2	63.0	18.3	70.5	65.6	74.3
Qwen2.5-VL-7B [3]	64.5	44.1	65.0	22.5	70.9	60.3	67.1
ArrowRL* [45]	67.5	50.1	65.0	20.2	71.7	60.1	66.2
<i>RL Post-Training of Qwen3-VL-4B</i>							
Qwen3-VL-4B (base) [2]	65.1	45.4	66.2	26.5	71.6	62.2	67.5
+ GRPO [13]	66.6	48.2	67.8	28.0	72.2	62.1	68.7
+ T-GRPO [9]	68.6	49.8	67.9	29.0	73.5	63.4	70.3
+ ArrowRL [45]	66.7	47.5	67.5	26.8	71.6	62.2	69.9
+ CRPO (Ours)	70.3 \uparrow _{5.2}	54.8 \uparrow _{9.4}	69.8 \uparrow _{3.6}	31.7 \uparrow _{5.2}	74.2 \uparrow _{2.6}	63.0 \uparrow _{0.8}	68.6 \uparrow _{1.1}
<i>RL Post-Training of Qwen3-VL-8B</i>							
Qwen3-VL-8B (base) [2]	68.2	50.4	67.8	27.8	75.1	64.9	68.7
+ GRPO [13]	69.4	52.4	69.8	30.5	75.5	64.5	69.1
+ T-GRPO [9]	70.9	54.5	70.3	32.5	75.4	65.0	69.5
+ ArrowRL [45]	69.6	52.2	69.3	29.3	74.9	65.1	69.7
+ CRPO (Ours)	72.5 \uparrow _{4.3}	58.1 \uparrow _{7.7}	71.7 \uparrow _{3.9}	36.0 \uparrow _{8.2}	77.4 \uparrow _{2.3}	65.6 \uparrow _{0.7}	69.7 \uparrow _{1.0}

with human labels on a 200-sample audit at 94% accuracy. Training takes place on 32 NVIDIA H20 GPUs. The full data composition, reward definitions, hyperparameter table, router prompt, and per-source classification statistics are provided in Appendices B.1, C, and B.2.

5.2 Main Results

Table 1 summarizes the comparison on the five benchmarks. Three observations stand out.

(1) CRPO outperforms all RL baselines on every spatiotemporal-sensitive benchmark. Compared with T-GRPO, the strongest competing RL method on the Qwen3-VL-4B backbone, CRPO improves DyBench P-Acc by +5.0 and TimeBlind I-Acc by +2.7, with consistently smaller but still positive gains on the standard-accuracy variants. The disproportionate gain on the paired metrics is the signature of reduced shortcut reliance, since prior methods can win an extra question on either side of a counterfactual pair without ever flipping their answer. Figure 4 illustrates this on a representative reversed pair, where the baseline Qwen3-VL returns the same prediction for both temporal orderings while CRPO flips its answer to match each ground truth. **(2) CRPO does not sacrifice general video understanding.** On the 4B backbone, CRPO improves over GRPO on VideoMME and remains competitive with the other RL baselines on MVBench. On the 8B backbone, CRPO leads all RL baselines on both general benchmarks. The static-task reward in CRR explicitly encourages invariance, which helps maintain the policy’s performance on questions whose answers are independent of the spatiotemporal perturbation. **(3) CRPO scales to a larger backbone.** On Qwen3-VL-8B, CRPO again leads every RL baseline on the spatiotemporal-sensitive benchmarks, with substantial paired gains over the base model (DyBench P-Acc +7.7, TimeBlind I-Acc +8.2). The benefit of counterfactual relational reward is therefore not specific to small models.

5.3 More Analysis

Does CRPO benefit from the framework or from more data? Because CRPO doubles the number of rollouts seen per training step (one original branch plus one counterfactual branch), a fair comparison must control for the data and compute budget. We add two GRPO controls: **GRPO (G \times 2)** doubles the rollout group size from 8 to 16 (matching CRPO’s effective rollout count per step), and **GRPO (Data \times 2)** duplicates each training sample so that the optimizer sees each prompt twice per epoch. The top half of Table 2 shows that neither control approaches CRPO. GRPO (G \times 2)

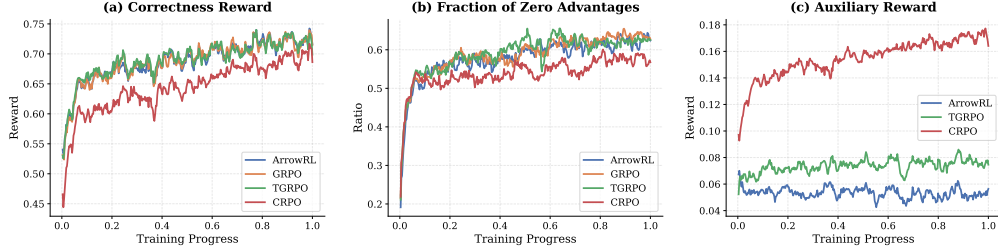


Figure 5: **Training dynamics of CRPO vs. RL baselines.** (a) correctness reward, (b) fraction of zero-advantage rollout groups, and (c) auxiliary reward.

Table 2: **Ablation on Qwen3-VL-4B.** Top: GRPO controls for rollout count and data exposure. Bottom: removing individual CRPO components.

RL Method	DyBench		TimeBlind		TempCompass	VideoMME	MVBench
	Acc	P-Acc	Acc	I-Acc	Acc	Acc	Acc
<i>Baseline</i>							
Qwen3-VL-4B (no RL)	65.1	45.4	66.2	26.5	71.6	62.2	67.5
<i>Data / Compute Controls</i>							
GRPO	66.6	48.2	67.8	28.0	72.2	62.1	68.7
GRPO (G×2)	68.5	50.2	68.5	29.0	74.0	62.3	70.2
GRPO (Data×2)	66.5	48.4	67.4	27.3	73.0	62.0	69.8
CRPO (Ours)	70.3	54.8	69.8	31.7	74.2	63.0	68.6
<i>Component Ablations (removing one element from CRPO)</i>							
w/o Spatial Flip	69.5	53.2	69.2	31.4	74.0	62.8	69.0
w/o Temporal Reversal	68.9	50.7	68.3	29.6	73.1	62.3	68.8
w/o R_{CRR}	69.3	51.2	68.8	30.5	73.1	63.0	67.5
w/o R_{behave}	69.6	52.7	69.1	31.4	73.5	62.7	69.1
w/o Counterfactual Branch	67.5	48.8	68.0	29.4	72.5	62.8	68.2
w/o Null Option	65.9	50.1	68.1	28.5	72.2	62.1	63.7

does close part of the gap on the standard accuracy of MVBench (and slightly exceeds CRPO there), but it fails to improve DyBench P-Acc and TimeBlind I-Acc to CRPO’s level, lagging behind by 4.6 and 2.7 respectively. GRPO (Data×2) provides essentially no benefit over the GRPO baseline. The gain of CRPO therefore cannot be explained by “twice the data” or “twice the rollouts”; it stems primarily from the cross-branch counterfactual reward.

Ablation study. The bottom half of Table 2 ablates each component of CRPO. (i) Removing the *spatial flip* or the *temporal reversal* transformation reduces P-Acc on DyBench by 1.6 and 4.1 respectively, confirming that both axes contribute and that temporal reversal is the more important one in our data mix. (ii) Removing the *cross-branch CRR* reward (R_{CRR}) drops DyBench P-Acc by 3.6, while removing only the *behavioral* reward R_{behave} on the counterfactual branch causes a smaller drop (−2.1). This shows that the *relational* signal across branches, not the per-branch behavior label, is the dominant source of CRPO’s gain. (iii) Removing the entire *counterfactual branch* (keeping only R_{CRR} as an auxiliary score for original-branch rollouts, similar in spirit to T-GRPO and ArrowRL) drops DyBench P-Acc by 6.0 to 48.8, essentially regressing to the level of the strongest RL baseline. This confirms that the *dual-branch optimization*, not just an auxiliary reward, is essential. (iv) Removing the *Null Option* produces a P-Acc that is reasonable on DyBench but causes the largest drop on MVBench (−4.9), because counterfactual rollouts on multiple-choice questions can no longer express the “the correct answer is not among the options” state and are pushed toward arbitrary wrong choices.

Training-curve analysis. Figure 5 compares the training dynamics of CRPO, GRPO, T-GRPO, and ArrowRL. Three observations stand out. **(a) Correctness reward.** GRPO, T-GRPO, and ArrowRL ramp up the correctness reward of the original branch very quickly, reaching ≈ 0.70 within the first 20% of training. CRPO’s correctness reward rises more slowly at the beginning, likely because the counterfactual branch and CRR make shortcut-based reward acquisition less effective

and encourage the policy to use spatiotemporal information. By the end of training, CRPO converges to a similar correctness level (≈ 0.71). **(b) Fraction of zero advantages.** The fraction of rollout groups with all-equal rewards (and therefore zero advantage) is consistently lower for CRPO, because the counterfactual branch’s R_{behave} introduces genuine intra-group variance even when the original branch is fully correct, providing richer learning signal per step. **(c) Auxiliary reward.** The auxiliary temporal-aware rewards used by T-GRPO and ArrowRL stay low and roughly flat throughout training, a phenomenon we attribute to their reward signals being cancelled during per-group advantage normalization (see Appendix F). In contrast, CRPO’s CRR reward grows steadily from 0.09 to 0.17, showing that the policy is actively learning to satisfy the counterfactual relation.

6 Conclusion

We present **CRPO**, a dual-branch GRPO framework that explicitly trains Video LLMs to be *spatiotemporally sensitive*. The key idea is the **Counterfactual Relation Reward**, which rewards the model when its answers on a video and a controlled counterfactual exhibit equivariance for spatiotemporal questions and invariance for static ones, thereby providing a direct training signal that is difficult for single-frame or language shortcuts to satisfy consistently. We also introduce **DyBench**, a paired counterfactual benchmark with a strict pair-accuracy metric for measuring this property. Experiments across DyBench, TimeBlind, TempCompass, VideoMME, and MVBench validate the effectiveness of CRPO. We hope that CRPO and DyBench together offer a useful step toward Video LLMs that are more sensitive to what changes in videos over time.

References

- [1] Emad Bahrami, Olga Zatsarynna, Parth Pathak, Sunando Sengupta, Juergen Gall, and Mohsen Fayyaz. Strive: Structured spatiotemporal exploration for reinforcement learning in video question answering. *arXiv preprint arXiv:2604.01824*, 2026.
- [2] Shuai Bai, Yuxuan Cai, Ruizhe Chen, Keqin Chen, Xionghui Chen, Zesen Cheng, Lianghao Deng, Wei Ding, Chang Gao, Chunjiang Ge, et al. Qwen3-vl technical report. *arXiv preprint arXiv:2511.21631*, 2025.
- [3] Shuai Bai, Keqin Chen, Xuejing Liu, Jialin Wang, Wenbin Ge, Sibao Song, Kai Dang, Peng Wang, Shijie Wang, Jun Tang, et al. Qwen2.5-vl technical report. *arXiv preprint arXiv:2502.13923*, 2025.
- [4] Mu Cai, Reuben Tan, Jianrui Zhang, Bocheng Zou, Kai Zhang, Feng Yao, Fangrui Zhu, Jing Gu, Yiwu Zhong, Yuzhang Shang, et al. Temporalbench: Benchmarking fine-grained temporal understanding for multimodal video models. *arXiv preprint arXiv:2410.10818*, 2024.
- [5] Jang Hyun Cho, Andrea Madotto, Effrosyni Mavroudi, Triantafyllos Afouras, Tushar Nagarajan, Muhammad Maaz, Yale Song, Tengyu Ma, Shuming Hu, Suyog Jain, et al. Perceptionlm: Open-access data and models for detailed visual understanding. *arXiv preprint arXiv:2504.13180*, 2025.
- [6] Christopher Clark, Jiayu Zhang, Zixian Ma, Jae Sung Park, Mohammadreza Salehi, Rohun Tripathi, Sangho Lee, Zhongzheng Ren, Chris Dongjoo Kim, YINUO Yang, et al. Molmo2: Open weights and data for vision-language models with video understanding and grounding. *arXiv preprint arXiv:2601.10611*, 2026.
- [7] Daniel Cores, Michael Dorkenwald, Manuel Mucientes, Cees GM Snoek, and Yuki M Asano. Lost in time: A new temporal benchmark for videollms. *arXiv preprint arXiv:2410.07752*, 2024.
- [8] Haodong Duan, Junming Yang, Yuxuan Qiao, Xinyu Fang, Lin Chen, Yuan Liu, Xiaoyi Dong, Yuhang Zang, Pan Zhang, Jiaqi Wang, et al. Vlmevalkit: An open-source toolkit for evaluating large multi-modality models. In *Proceedings of the 32nd ACM international conference on multimedia*, pages 11198–11201, 2024.
- [9] Kaituo Feng, Kaixiong Gong, Bohao Li, Zonghao Guo, Yibing Wang, Tianshuo Peng, Junfei Wu, Xiaoying Zhang, Benyou Wang, and Xiangyu Yue. Video-r1: Reinforcing video reasoning in mllms. In *NeurIPS*, 2025.

- [10] Kaituo Feng, Manyuan Zhang, Hongyu Li, Kaixuan Fan, Shuang Chen, Yilei Jiang, Dian Zheng, Peiwen Sun, Yiyuan Zhang, Haoze Sun, et al. Onethinker: All-in-one reasoning model for image and video. *arXiv preprint arXiv:2512.03043*, 2025.
- [11] Chaoyou Fu, Yuhan Dai, Yongdong Luo, Lei Li, Shuhuai Ren, Renrui Zhang, Zihan Wang, Chenyu Zhou, Yunhang Shen, Mengdan Zhang, et al. Video-mme: The first-ever comprehensive evaluation benchmark of multi-modal llms in video analysis. In *Proceedings of the IEEE/CVF conference on computer vision and pattern recognition*, pages 24108–24118, 2025.
- [12] Raghav Goyal, Samira Ebrahimi Kahou, Vincent Michalski, Joanna Materzynska, Susanne Westphal, Heuna Kim, Valentin Haebel, Ingo Fruend, Peter Yianilos, Moritz Mueller-Freitag, et al. The "something something" video database for learning and evaluating visual common sense. In *Proceedings of the IEEE international conference on computer vision*, pages 5842–5850, 2017.
- [13] Daya Guo, Dejian Yang, Haowei Zhang, Junxiao Song, Peiyi Wang, Qihao Zhu, Runxin Xu, Ruoyu Zhang, Shirong Ma, Xiao Bi, et al. Deepseek-r1 incentivizes reasoning in llms through reinforcement learning. *Nature*, 645(8081):633–638, 2025.
- [14] Wenyi Hong, Yean Cheng, Zhuoyi Yang, Weihang Wang, Lefan Wang, Xiaotao Gu, Shiyu Huang, Yuxiao Dong, and Jie Tang. Motionbench: Benchmarking and improving fine-grained video motion understanding for vision language models. In *Proceedings of the Computer Vision and Pattern Recognition Conference*, pages 8450–8460, 2025.
- [15] Jian Hu, Jason Klein Liu, Haotian Xu, and Wei Shen. Reinforce++: Stabilizing critic-free policy optimization with global normalization. *arXiv preprint arXiv:2501.03262*, 2025.
- [16] Lianghua Huang, Xin Zhao, and Kaiqi Huang. Got-10k: A large high-diversity benchmark for generic object tracking in the wild. *IEEE transactions on pattern analysis and machine intelligence*, 43(5):1562–1577, 2019.
- [17] Ming Kong, Xianzhou Zeng, Luyuan Chen, Yadong Li, Bo Yan, and Qiang Zhu. Mhbench: Demystifying motion hallucination in videollms. In *Proceedings of the AAAI Conference on Artificial Intelligence*, volume 39, pages 4401–4409, 2025.
- [18] Benno Krojer, Mojtaba Komeili, Candace Ross, Quentin Garrido, Koustuv Sinha, Nicolas Ballas, and Mahmoud Assran. A shortcut-aware video-qa benchmark for physical understanding via minimal video pairs. *arXiv preprint arXiv:2506.09987*, 2025.
- [19] Hilde Kuehne, Ali Arslan, and Thomas Serre. The language of actions: Recovering the syntax and semantics of goal-directed human activities. In *Proceedings of the IEEE conference on computer vision and pattern recognition*, pages 780–787, 2014.
- [20] Jie Lei, Tamara Berg, and Mohit Bansal. Revealing single frame bias for video-and-language learning. In *Proceedings of the 61st Annual Meeting of the Association for Computational Linguistics (Volume 1: Long Papers)*, pages 487–507, 2023.
- [21] Baiqi Li, Kangyi Zhao, Ce Zhang, Chancharik Mitra, Jean de Dieu Nyandwi, and Gedas Bertasius. Timeblind: A spatio-temporal compositionality benchmark for video llms. *arXiv preprint arXiv:2602.00288*, 2026.
- [22] Bo Li, Yuanhan Zhang, Dong Guo, Renrui Zhang, Feng Li, Hao Zhang, Kaichen Zhang, Peiyuan Zhang, Yanwei Li, Ziwei Liu, et al. Llava-onevision: Easy visual task transfer. *arXiv preprint arXiv:2408.03326*, 2024.
- [23] Chaoyu Li, Eun Woo Im, and Pooyan Fazli. Vidhalluc: Evaluating temporal hallucinations in multimodal large language models for video understanding. In *Proceedings of the IEEE/CVF Conference on Computer Vision and Pattern Recognition*, pages 13723–13733, 2025.
- [24] Kunchang Li, Yali Wang, Yinan He, Yizhuo Li, Yi Wang, Yi Liu, Zun Wang, Jilan Xu, Guo Chen, Ping Luo, et al. Mvbench: A comprehensive multi-modal video understanding benchmark. In *Proceedings of the IEEE/CVF Conference on Computer Vision and Pattern Recognition*, pages 22195–22206, 2024.

- [25] Xinhao Li, Ziang Yan, Desen Meng, Lu Dong, Xiangyu Zeng, Yinan He, Yali Wang, Yu Qiao, Yi Wang, and Limin Wang. Videochat-r1: Enhancing spatio-temporal perception via reinforcement fine-tuning. *arXiv preprint arXiv:2504.06958*, 2025.
- [26] Yun Li, Yiming Zhang, Tao Lin, XiangRui Liu, Wenxiao Cai, Zheng Liu, and Bo Zhao. Stibench: Are mllms ready for precise spatial-temporal world understanding? In *Proceedings of the IEEE/CVF International Conference on Computer Vision*, pages 5622–5632, 2025.
- [27] Haotian Liu, Chunyuan Li, Qingyang Wu, and Yong Jae Lee. Visual instruction tuning. *Advances in neural information processing systems*, 36:34892–34916, 2023.
- [28] Shuming Liu, Mingchen Zhuge, Changsheng Zhao, Jun Chen, Lemeng Wu, Zechun Liu, Chenchen Zhu, Zhipeng Cai, Chong Zhou, Haozhe Liu, et al. Videoauto-r1: Video auto reasoning via thinking once, answering twice. *arXiv preprint arXiv:2601.05175*, 2026.
- [29] Yuanxin Liu, Shicheng Li, Yi Liu, Yuxiang Wang, Shuhuai Ren, Lei Li, Sishuo Chen, Xu Sun, and Lu Hou. Tempcompass: Do video llms really understand videos? In *Findings of the Association for Computational Linguistics: ACL 2024*, pages 8731–8772, 2024.
- [30] Zihe Liu, Jiashun Liu, Yancheng He, Weixun Wang, Jiaheng Liu, Ling Pan, Xinyu Hu, Shaopan Xiong, Ju Huang, Jian Hu, et al. Part i: Tricks or traps? a deep dive into rl for llm reasoning. *arXiv preprint arXiv:2508.08221*, 2025.
- [31] Jinyoung Park, Jeehye Na, Jinyoung Kim, and Hyunwoo J Kim. Deepvideo-r1: Video reinforcement fine-tuning via difficulty-aware regressive grpo. In *NeurIPS*, 2025.
- [32] Sundar Pichai, Demis Hassabis, and Koray Kavukcuoglu. A new era of intelligence with gemini 3, 2025. URL <https://blog.google/intl/en-africa/company-news/outreach-and-initiatives/a-new-era-of-intelligence-with-gemini-3/>.
- [33] Xiaoqian Shen, Yunyang Xiong, Changsheng Zhao, Lemeng Wu, Jun Chen, Chenchen Zhu, Zechun Liu, Fanyi Xiao, Balakrishnan Varadarajan, Florian Bordes, et al. Longvu: Spatiotemporal adaptive compression for long video-language understanding. *arXiv preprint arXiv:2410.17434*, 2024.
- [34] Jiapeng Shi, Junke Wang, Zuyao You, Bo He, and Zuxuan Wu. Videoloom: A video large language model for joint spatial-temporal understanding. *arXiv preprint arXiv:2601.07290*, 2026.
- [35] Yan Shu, Zheng Liu, Peitian Zhang, Minghao Qin, Junjie Zhou, Zhengyang Liang, Tiejun Huang, and Bo Zhao. Video-xl: Extra-long vision language model for hour-scale video understanding. In *Proceedings of the Computer Vision and Pattern Recognition Conference*, pages 26160–26169, 2025.
- [36] Aaditya Singh, Adam Fry, Adam Perelman, Adam Tart, Adi Ganesh, Ahmed El-Kishky, Aidan McLaughlin, Aiden Low, AJ Ostrow, Akhila Ananthram, et al. Openai gpt-5 system card. *arXiv preprint arXiv:2601.03267*, 2025.
- [37] Enxin Song, Wenhao Chai, Guan hong Wang, Yucheng Zhang, Haoyang Zhou, Feiyang Wu, Haozhe Chi, Xun Guo, Tian Ye, Yanting Zhang, et al. Moviechat: From dense token to sparse memory for long video understanding. In *Proceedings of the IEEE/CVF Conference on Computer Vision and Pattern Recognition*, pages 18221–18232, 2024.
- [38] Sebastian Stein and Stephen J McKenna. Combining embedded accelerometers with computer vision for recognizing food preparation activities. In *Proceedings of the 2013 ACM international joint conference on Pervasive and ubiquitous computing*, pages 729–738, 2013.
- [39] Haozhe Wang, Chao Qu, Zuming Huang, Wei Chu, Fangzhen Lin, and Wenhua Chen. VI-rethinker: Incentivizing self-reflection of vision-language models with reinforcement learning. *arXiv preprint arXiv:2504.08837*, 2025.
- [40] Qi Wang, Yanrui Yu, Ye Yuan, Rui Mao, and Tianfei Zhou. Videorf1: Incentivizing video reasoning capability in mllms via reinforced fine-tuning. In *NeurIPS*, 2025.

- [41] Weihan Wang, Zehai He, Wenyi Hong, Yean Cheng, Xiaohan Zhang, Ji Qi, Ming Ding, Xiaotao Gu, Shiyu Huang, Bin Xu, et al. Lvbench: An extreme long video understanding benchmark. In *Proceedings of the IEEE/CVF International Conference on Computer Vision*, pages 22958–22967, 2025.
- [42] Weiyun Wang, Zhangwei Gao, Lixin Gu, Hengjun Pu, Long Cui, Xingguang Wei, Zhaoyang Liu, Linglin Jing, Shenglong Ye, Jie Shao, et al. Internvl3.5: Advancing open-source multimodal models in versatility, reasoning, and efficiency. *arXiv preprint arXiv:2508.18265*, 2025.
- [43] Xiyao Wang, Zhengyuan Yang, Chao Feng, Hongjin Lu, Linjie Li, Chung-Ching Lin, Kevin Lin, Furong Huang, and Lijuan Wang. Sota with less: Mcts-guided sample selection for data-efficient visual reasoning self-improvement. *arXiv preprint arXiv:2504.07934*, 2025.
- [44] Ziyue Wang, Sheng Jin, Zhongrong Zuo, Jiawei Wu, Han Qiu, Qi She, Hao Zhang, and Xudong Jiang. Video-kr: Reinforcing video reasoning via key token attribution. *arXiv preprint arXiv:2601.19686*, 2026.
- [45] Zihui Xue, Mi Luo, and Kristen Grauman. Seeing the arrow of time in large multimodal models. In *NeurIPS*, 2025.
- [46] Kexin Yi, Chuang Gan, Yunzhu Li, Pushmeet Kohli, Jiajun Wu, Antonio Torralba, and Joshua B Tenenbaum. Clevrer: Collision events for video representation and reasoning. *arXiv preprint arXiv:1910.01442*, 2019.
- [47] En Yu, Kangheng Lin, Liang Zhao, Yana Wei, Zining Zhu, Haoran Wei, Jianjian Sun, Zheng Ge, Xiangyu Zhang, Jingyu Wang, et al. Unhackable temporal rewarding for scalable video mllms. *arXiv preprint arXiv:2502.12081*, 2025.
- [48] Qiyang Yu, Zheng Zhang, Ruofei Zhu, Yufeng Yuan, Xiaochen Zuo, Yu Yue, Weinan Dai, Tiantian Fan, Gaohong Liu, Lingjun Liu, et al. Dapo: An open-source llm reinforcement learning system at scale. *arXiv preprint arXiv:2503.14476*, 2025.
- [49] Yuqian Yuan, Hang Zhang, Wentong Li, Zesen Cheng, Boqiang Zhang, Long Li, Xin Li, Deli Zhao, Wenqiao Zhang, Yueting Zhuang, et al. Videorefer suite: Advancing spatial-temporal object understanding with video llm. In *Proceedings of the Computer Vision and Pattern Recognition Conference*, pages 18970–18980, 2025.
- [50] Boqiang Zhang, Kehan Li, Zesen Cheng, Zhiqiang Hu, Yuqian Yuan, Guanzheng Chen, Sicong Leng, Yuming Jiang, Hang Zhang, Xin Li, et al. Videollama 3: Frontier multimodal foundation models for image and video understanding. *arXiv preprint arXiv:2501.13106*, 2025.
- [51] Yuanhan Zhang, Jinming Wu, Wei Li, Bo Li, Zejun Ma, Ziwei Liu, and Chunyuan Li. Llava-video: Video instruction tuning with synthetic data. *arXiv preprint arXiv:2410.02713*, 2024.
- [52] Yilun Zhao, Haowei Zhang, Lujing Xie, Tongyan Hu, Guo Gan, Yitao Long, Zhiyuan Hu, Weiyuan Chen, Chuhan Li, Zhijian Xu, et al. Mmvu: Measuring expert-level multi-discipline video understanding. In *Proceedings of the Computer Vision and Pattern Recognition Conference*, pages 8475–8489, 2025.
- [53] Kejian Zhu, Zhuoran Jin, Hongbang Yuan, Jiachun Li, Shangqing Tu, Pengfei Cao, Yubo Chen, Kang Liu, and Jun Zhao. Mmr-v: What’s left unsaid? a benchmark for multimodal deep reasoning in videos. *arXiv preprint arXiv:2506.04141*, 2025.
- [54] Orr Zohar, Xiaohan Wang, Yann Dubois, Nikhil Mehta, Tong Xiao, Philippe Hansen-Estruch, Licheng Yu, Xiaofang Wang, Felix Juefei-Xu, Ning Zhang, et al. Apollo: An exploration of video understanding in large multimodal models. In *Proceedings of the Computer Vision and Pattern Recognition Conference*, pages 18891–18901, 2025.

A DyBench: Construction, Comparison, and Detailed Analysis

A.1 Design principle and held-out evaluation

The design of DyBench follows the recent observation that Video LLMs frequently solve dynamic questions through static shortcuts [18, 21]. Following the temporal-minimal-pair protocol popularized by TimeBlind [21], every DyBench item is built as a pair (v, v') of videos that share the same scene and objects but differ along a single dynamic axis. The matching question q has different correct answers for v and v' , so a model that exploits a single keyframe or a language prior cannot simultaneously satisfy both. Pair accuracy then reports the fraction of pairs answered correctly on *both* sides, providing a much stricter measure of dynamic understanding than per-question accuracy.

DyBench is also a strict out-of-distribution evaluation. None of its source datasets (something-something-v2 [12], MHBench [17], GOT-10k [16], the Breakfast cooking dataset [19], etc.) appear in the training pool used by any of the RL methods we benchmark. Our training pool consists of Video-R1, TVBench, STI-Bench, and MMR-VBench (Appendix B). Every gain reported on DyBench therefore reflects *generalization* of spatiotemporal sensitivity acquired during RL training rather than memorization of the evaluation distribution.

A.2 Sub-task construction

Sub-task 1: Reversible Dynamics. We collect actions whose semantics flip under temporal reversal. The action vocabulary covers humans, animals, and plants:

- *Human actions* sourced from MHBench [17], something-something-v2 [12], and web-crawled clips: opening↔closing, picking up↔putting down, lifting↔throwing, hanging↔taking down, raising↔lowering, folding↔unfolding, pushing↔pulling, plugging in↔unplugging, zipping↔unzipping, rolling↔unrolling, tying↔untying, fastening↔unfastening, turning on↔turning off, getting in↔getting out, putting on↔taking off, inserting↔removing, stacking↔unstacking, sitting/lying/kneeling/squatting down↔standing up, inflating↔deflating, tightening↔loosening, assembling↔disassembling, leaning forward↔leaning back, bowing↔straightening up, drawing curtain open↔closed, walking forward↔backward, opening eyes↔closing eyes.
- *Animal/plant actions* sourced from web-crawled clips: standing up↔lying down, jumping up↔landing, jumping into water↔leaping out, spreading wings↔folding wings, ears up↔flattened, arching back↔relaxing, retracting into shell↔extending out, stretching neck out↔retracting, opening mouth↔closing, extending tongue↔retracting, elephant raising trunk↔lowering trunk, raising head↔lowering head, flower blooming↔closing, leaf unfolding↔folding.

For each source clip we generate v (forward play) and v' (reverse play). The question asks “Which of the following best describes the action in the video?” with options drawn from the forward action, the reversed action, and a distractor. The answer flips between v and v' .

Sub-task 2: Moving Direction. We use object-tracking videos from GOT-10k [16] and motion-direction questions from CLEVRER [46]. For each source clip we generate v (original) and v' (horizontally flipped, optionally also temporally reversed). The question asks “In what direction is the [object] moving?” with the four standard direction options. For tracking videos with non-axial motion (e.g., diagonals), the option set is augmented with the four diagonals.

Sub-task 3: Event Sequence. We assemble pairs of two-event composite videos from four sources, including Breakfast [19], 50Salads [38], VIDHALLUC [23] and TempCompass [29]. For Breakfast and 50Salads, we follow the original action annotations and sample two non-adjacent action segments per video (each ≤ 30 s). The two segments are concatenated to form v and concatenated in the reverse order to form v' . For VIDHALLUC, we use cached DINO features to find the splice point, keeping only those clips with exactly one detected splice. Each clip is then re-spliced in reverse order to form v' .

Quality control. Every pair undergoes manual verification of (i) static-content consistency between v and v' , (ii) temporal minimality (no other temporal cue differs), and (iii) unambiguous correctness of the answer for both videos. Pairs that fail any check are discarded.

A.3 Comparison with existing video benchmarks

Table 3 compares DyBench with widely used video benchmarks along four dimensions: scale, video length, domain focus, and whether the benchmark uses adversarial pair construction. DyBench is most closely related to TimeBlind [21] in spirit, since both use minimal pair construction and paired evaluation, but DyBench focuses specifically on three motion-aware sub-tasks (reversible dynamics, moving direction, and event sequence) and reports pair accuracy as the primary metric. In addition, the DyBench dataset is much larger.

Table 3: DyBench vs. existing video benchmarks. “Adversarial” means each item is paired with a counter-example designed to flip the answer.

Benchmark	#Videos / #QAs	Length	Domain	Adversarial
MVBench [24]	4,000 / 4,000	short	general	No
VideoMME [11]	900 / 2,700	short, long	general	No
LVBench [41]	103 / 1,549	long	general	No
TempCompass [29]	410 / 1,580	short	dynamic	Yes
TemporalBench [4]	2,000 / 10,000	short, long	dynamic	No
MotionBench [14]	5,385 / 8,052	short	human action	No
MHBench [17]	1,200 / 3,600	short	human action	Yes
TimeBlind [21]	1,200 / 2,400	short	dynamic	Yes
DyBench (Ours)	3,014 / 3,014	short	dynamic	Yes

A.4 Shortcut-isolation analysis

A central design goal of DyBench is to make static shortcuts ineffective under paired evaluation. We verify this by re-evaluating models under three handicapped input settings, in the spirit of the shortcut analyses of TimeBlind [21] and MVP [18].

- **Single Frame.** The model receives only a single, randomly sampled frame from each video.
- **Shuffled Frames.** The model receives all 32 frames but in a uniformly random order, destroying temporal structure while preserving every static cue.
- **Text Only.** The model receives the question and options without any visual input.

A benchmark that is genuinely diagnostic of spatiotemporal understanding should drive accuracy to near-chance under all three settings. Table 4 reports the results. Because DyBench mixes 2-, 3-, and 4-way questions, the random-chance overall is 35.1% for Acc and 13.3% for P-Acc; per sub-task, the chance values are 33.3%/11.1% for Reversible Dynamics (3-way), 25.0%/6.3% for Moving Direction (4-way), and 50.0%/25.0% for Event Sequence (binary).

Table 4: **Shortcut-isolation analysis on DyBench.** “Full Video” is the standard 32-frame setting reproduced from Table 1; the other three columns are handicapped inputs that destroy temporal information.

Model	Full Video		Single Frame		Shuffled Frames		Text Only	
	Acc	P-Acc	Acc	P-Acc	Acc	P-Acc	Acc	P-Acc
GPT-5.1	63.7	44.9	39.9	5.1	30.5	3.0	32.8	2.6
Gemini-3.1-Pro	82.2	71.7	43.3	6.8	41.6	7.7	42.8	6.1
Qwen3-VL-8B	68.2	50.4	35.1	7.2	42.3	10.2	27.7	0.4
+ CRPO (Ours)	72.5	58.1	37.9	7.4	44.3	13.2	36.8	1.1
Random chance	35.1	13.3	35.1	13.3	35.1	13.3	35.1	13.3

We find that **under every handicapped input, all models collapse to or below chance on the strict pair metric.** CRPO drops from 58.1 P-Acc on the full video to 7.4 (Single Frame), 13.2

(Shuffled Frames), and 1.1 (Text Only), well below the 13.3 chance level for two of the three settings. The same pattern holds for GPT-5.1 (P-Acc collapses from 44.9 to ≤ 5.1), Gemini-3.1-Pro and the Qwen3-VL-8B baseline. This validates DyBench as a benchmark that genuinely requires temporal information, since shuffling frames, removing all but one frame, or removing the video entirely all destroy the signal needed to solve it. Note that the Text-Only P-Acc values are small but not exactly zero because certain DyBench sub-tasks present different option sets for the two sides of a pair (e.g., reversed option order in Moving Direction), so the model sees slightly different text prompts and can occasionally produce different answers even without visual input.

A.5 Per-sub-task breakdown

Table 5 decomposes DyBench accuracy into the three sub-tasks introduced in Sec. 4.

Table 5: **Per-sub-task DyBench results.** Both per-question accuracy (Acc) and pair accuracy (P-Acc) are reported on each sub-task.

Model	Reversible Dynamics		Moving Direction		Event Sequence		Overall	
	Acc	P-Acc	Acc	P-Acc	Acc	P-Acc	Acc	P-Acc
GPT-5.1	80.7	66.0	31.2	9.6	78.5	57.0	63.7	44.9
Gemini-3.1-Pro	96.1	92.3	57.7	36.8	91.9	84.3	82.2	71.7
Qwen3-VL-4B (base)	78.9	64.3	40.1	18.0	75.4	51.1	65.1	45.4
+ GRPO	82.0	67.3	39.0	19.0	77.9	56.0	66.6	48.2
+ T-GRPO	82.0	68.3	44.7	21.8	78.3	57.0	68.6	49.8
+ ArrowRL	80.8	47.5	40.1	17.2	78.5	57.0	66.7	47.5
+ CRPO (Ours)	86.8	77.7	41.8	21.0	81.1	62.7	70.3	54.8
Qwen3-VL-8B (base)	83.3	70.8	40.8	18.2	79.5	59.7	68.2	50.4
+ GRPO	84.0	71.8	41.4	17.6	82.4	66.3	69.4	52.4
+ T-GRPO	85.5	74.3	43.5	20.0	83.3	67.6	70.9	54.5
+ ArrowRL	84.2	71.2	42.0	19.4	82.1	64.6	69.6	52.2
+ CRPO (Ours)	89.8	81.5	41.7	19.8	85.0	70.5	72.5	58.1
Random chance	33.3	11.1	25.0	6.3	50.0	25.0	35.1	13.3

Three observations stand out. **(i) CRPO delivers its largest absolute gains on *Reversible Dynamics* and *Event Sequence***, the two sub-tasks that most directly require temporal reasoning. On the 4B backbone, CRPO improves Reversible Dynamics by +7.9 Acc / +13.4 P-Acc and Event Sequence by +5.7 Acc / +11.6 P-Acc over the baseline, more than doubling the typical gain of GRPO on these sub-tasks. **(ii) Moving Direction remains hard for all open-source models**, with even the best 8B variant scoring around 42 Acc / 20 P-Acc; this sub-task is dominated by 4-way questions whose answers depend on tracking subtle direction cues across frames, and is where Gemini-3.1-Pro keeps a sizeable lead. **(iii) The strict pair-accuracy gap between models and chance is much larger than the standard-accuracy gap**: for example, on Reversible Dynamics CRPO-8B reaches 89.8 Acc ($2.7\times$ chance) versus 81.5 P-Acc ($7.3\times$ chance), confirming that pair accuracy is a far more discriminative signal of genuine spatiotemporal reasoning.

B Training Data and Implementation Details

B.1 Training data and reward functions

Data sources. The training corpus combines text, image, and video QA, summarized in Table 6. The dual-branch counterfactual framework of CRPO is applied only to video samples, where spatial and temporal perturbations are meaningful. Text and image samples are trained with standard single-branch GRPO. Following standard practice, samples for which the base model is either always correct or always wrong across 8 base-model rollouts are filtered out, since they carry no signal under group-relative advantages. The video subset contains 21,165 samples after filtering, whose distribution across Task Router categories is reported in Appendix C.

Table 6: Training data composition.

Modality	Sources	Approx. size
Text	DAPO-Math [48]	6.4K
Image	VIRL [39], ThinkLite-VL-Hard [43]	27.5K
Video	Video-R1 [9], TVBench [7], STI-Bench [26], MMR-VBench [53]	21.2K

Reward functions. We use two standard reward terms shared by all RL methods, namely a QA-style *accuracy* reward and a *format* reward. The accuracy reward is binary, with math problems verified by `math-verify` and other QA checked by case-folded, whitespace-stripped string match. The format reward is binary and enforces a strict regex of one `<think>` block followed by a single `\boxed{}`. CRPO additionally introduces R_{CRR} and R_{behave} as defined in Sec. 3, and the four CRR/behave reward components are visualized in Figure 7 of Appendix D.

Training prompt. All RL methods (CRPO and the baselines) use the following RL-with-Thinking system prompt during training.

Training System Prompt

You are a helpful assistant. **FIRST**, think through the reasoning process as an internal monologue, and **THEN** provide the final answer. The reasoning process **MUST** be enclosed within `<think>` `</think>` tags, and the final answer **MUST** be wrapped in `\boxed{}`.

For multiple-choice questions, the option list is appended to the user prompt together with the appended “None of the above” (Sec. 3, Null Option).

B.2 Hyperparameters

Table 7 lists the key hyperparameters used by all RL methods (GRPO, T-GRPO, ArrowRL, and CRPO). Hyperparameters that differ between methods are limited to the CRPO-specific block at the bottom of the table.

Evaluation toolkit. All evaluations are run with the public VLMEvalKit [8] toolkit³ with its default configuration of 32 uniformly sampled frames per video for video benchmarks. We do not change any benchmark-side prompts or option ordering, and we use greedy decoding.

B.3 Baseline RL algorithms

For a fair comparison, all RL post-training baselines (GRPO, T-GRPO, ArrowRL) are reproduced under the same backbone, training data, and shared hyperparameters as CRPO. They differ only in the RL algorithm. We reimplement each baseline strictly following its original paper.

GRPO [13]. The vanilla baseline. For each prompt, the policy generates $G=8$ rollouts, and each rollout receives the standard correctness reward $R_{\text{correct}} = \mathbb{I}[o = o^*]$ plus the format reward R_{format} . Advantages are computed by subtracting the group mean reward and normalizing by the group standard deviation, and the policy is updated with the clipped GRPO surrogate objective.

T-GRPO [9]. Following Video-R1, for each prompt we additionally generate a second group of $G=8$ rollouts on a frame-shuffled version of the input video. Let p and \tilde{p} denote the fraction of correct rollouts in the ordered and shuffled groups, respectively. We add a temporal reward $r_t = \alpha \cdot \mathbb{I}[p \geq \tilde{p}]$ with $\alpha = 0.3$ to each correct rollout in the ordered group. Following the original paper, the shuffled group is used only to compute \tilde{p} and does *not* contribute to the policy gradient, so the optimization is effectively single-branch. The temporal reward is applied only to video samples.

ArrowRL [45]. Following the original paper, for each prompt we generate one rollout group on the original video and a single reference response \tilde{o} on the temporally reversed video. The reward for each original-video rollout o_i combines a fidelity term and a reverse term, $r_i = r_i^{\text{fid}} + \alpha_i \cdot r_i^{\text{rev}}$, where

³<https://github.com/open-compass/VLMEvalKit>

Table 7: Key training hyperparameters. The first block is shared by all RL baselines; the second block is CRPO-specific.

Hyperparameter	Value
<i>Shared (all RL methods)</i>	
Backbone	Qwen3-VL-4B / 8B-Instruct [2]
Tunable modules	LLM + multimodal projector (vision encoder frozen)
Optimizer	AdamW (fused), $\beta_1=0.9$, $\beta_2=0.999$, weight decay 0.01
Learning rate / schedule	1×10^{-6} , constant with warmup
KL coefficient β	0.01
Max gradient norm	1.0
Batch size (per device)	4
Generation steps per update	8
Rollouts per group G	8
Max prompt / completion length	8192 / 2048
Sampled frames per video	32 (uniform)
Pixel budget per video	$\leq 2048 \times 32 \times 32$
Pixel budget per frame	$[16, 768] \times 32 \times 32$
Epochs	1
Precision	BF16, ZeRO-3, gradient checkpointing
Rollout backend	vLLM (colocate, TP=8, GPU mem util. 0.45)
Hardware	32 NVIDIA H20 GPUs (4 nodes \times 8)
<i>CRPO-specific</i>	
Cross-branch CRR weight $\lambda_d=\lambda_s$	0.3
Counterfactual branch weight w_{aug}	0.5
Counterfactual transformations	horizontal flip; temporal reversal

$r_i^{\text{fid}} = \mathbb{I}[o_i = o^*]$ for multiple-choice questions, $r_i^{\text{rev}} = 1 - \mathbb{I}[o_i = \tilde{o}]$ penalizes rollouts that mirror the reverse-conditioned response, and α_i is a dynamic weight set to $\alpha = 0.25$ for AoT-sensitive samples ($\tilde{o} = o^*$) and 0 otherwise ($\tilde{o} \neq o^*$). The reversed video is used only to compute \tilde{o} for reward shaping and does not contribute policy gradients.

C Task Router

Classification model. The Task Router is run *offline* once on the entire training set with DeepSeek-R1, a text-only reasoning model. We deliberately use a reasoning-style model rather than a stronger multimodal model because the classification only requires textual imagination over the question and options. We observed that even a moderate reasoning model is sufficient for $\sim 94\%$ accuracy.

Prompt template. The full prompt template is reproduced below. It is the verbose implementation of the two imagination questions shown in Figure 2 (right panel), with detailed criteria for what counts as a YES versus a NO under each test. Since the Task Router classifies only video samples, the prompt is designed around video-specific transformations (horizontal flip and temporal reversal).

Task Router Prompt (used with DeepSeek-R1)

Task. Classify this VQA item into [Temporal, Spatial, Spatiotemporal, Static] based on two transformation tests.

1. Horizontal Flip Test (Spatial Sensitivity). If the video is mirrored horizontally (Left \leftrightarrow Right):

- **YES (Change):** queries about left/right, clockwise/counter-clockwise, or horizontal orientation.
- **NO (No Change):** queries about verticality (top/bottom, high/low, tall/short), color, identity, size, or count.

2. Time-Reversal Test (Temporal Sensitivity). If the video is played in REVERSE (frames played backwards, time flows backward):

- **YES (Change)**: directional actions where forward \neq backward (opening \rightarrow closing, picking up \rightarrow putting down, entering \rightarrow exiting); questions about FIRST/LAST or BEFORE/AFTER; questions about cause/result of a sequence.
- **NO (No Change)**: counting, identity/color/material/shape/size, persistent states or attributes, motion direction or speed that are symmetric under reversal.

Decision Matrix.

- Spatial: Flip **YES** AND Time-Reversal **NO**.
- Temporal: Flip **NO** AND Time-Reversal **YES**.
- Spatiotemporal: **both YES**.
- Static: **both NO**.

Data. Q: {problem} Options: {options} A: {solution}

Instructions. First, briefly reason through the two tests. Then, on the very last line, output **ONLY** one word from {Temporal, Spatial, Spatiotemporal, Static}.

Statistics on the training set. Table 8 reports the per-source distribution. The video subset is dominated by Temporal questions (73.6%), reflecting that most existing video QA data is action- or event-centric. Pure Spatial questions are rare (2.3%), and Spatiotemporal questions, which require both axes, account for 4.1%. The Static category (20.0%) covers static questions about presence, count, color, etc.

Table 8: Task Router classification statistics on the video training set (21,165 samples).

Dataset	Temporal	Spatial	Spatiotmp.	Static	Total
Video-R1	14,359 (80.8%)	173 (1.0%)	310 (1.7%)	2,936 (16.5%)	17,778
TVBench	979 (70.9%)	2 (0.1%)	238 (17.2%)	161 (11.7%)	1,380
STI-Bench	81 (5.3%)	313 (20.5%)	319 (20.8%)	817 (53.4%)	1,530
MMR-VBench	163 (34.2%)	3 (0.6%)	1 (0.2%)	310 (65.0%)	477
Total	15,582 (73.6%)	491 (2.3%)	868 (4.1%)	4,224 (20.0%)	21,165

Validation by manual relabeling. To verify the router’s quality, we randomly sampled 200 video QA examples and manually re-labeled them by watching each video together with the question and options. The router agreed with human labels on 188 of 200 cases (**94%**). Of the 12 disagreements, 8 were borderline cases between Temporal and Spatiotemporal (the human labeller felt that the action also depended on left/right cues), 3 were Static samples mistakenly classified as Temporal, and 1 was a counting question mislabeled as Spatial. We note that router misclassifications do produce incorrect reward signals (e.g., a dynamic question classified as static would be rewarded for invariance instead of equivariance). However, the observed error rate of 6% is low and the majority of errors are borderline Temporal/Spatiotemporal confusions, which still receive a correct transformation type (temporal reversal applies to both categories). The 4 remaining errors (3 static \rightarrow temporal, 1 spatial misclassification) affect a negligible fraction of training samples.

Example router outputs. Figure 6 shows representative router outputs across the four categories. Each panel shows one video, the question and options, the ground-truth answer, and the router’s category assignment with its short reasoning trace. We additionally reproduce six complete textual examples below, covering all four categories (Temporal, Spatial, Spatiotemporal, and Static), including the full reasoning chains produced by DeepSeek-R1.

Example 1 • Source: STAR • Decision: Temporal

Q: What did the person do with the clothes?
Options: (A) Lied on. (B) Took. (C) Put down. (D) Washed.
A: C.

Reasoning.

1. *Horizontal Flip Test (Spatial Sensitivity).* If we mirror the video horizontally (left becomes right), the action of the person putting down the clothes remains exactly the same. The question does not rely on left/right orientation or horizontal positioning. **NO (No Change).**

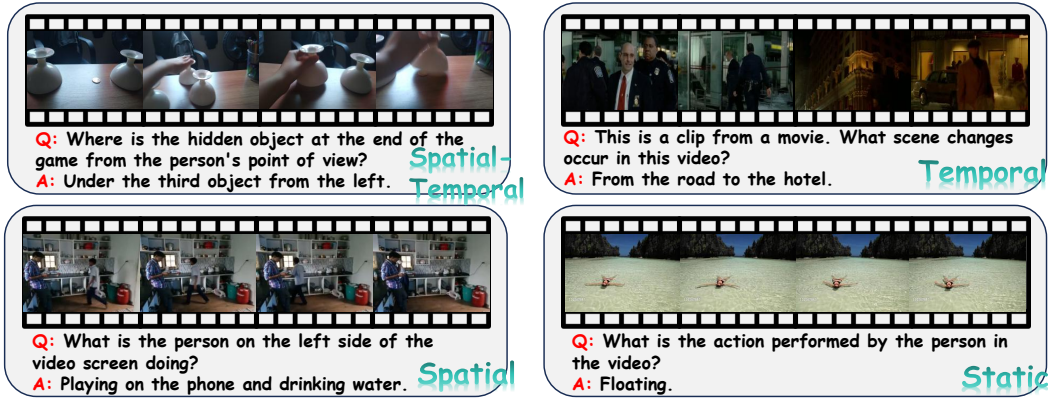


Figure 6: **Task Router** output examples after applying the prompt above to randomly sampled videos. The router outputs a category label together with a short text-only reasoning chain.

2. *Time-Reversal Test (Temporal Sensitivity)*. If we play the video in reverse, “putting down” the clothes would look like the person is picking them up or “taking” them (Option B). Because the direction of time fundamentally changes the nature of this action, the correct answer would change. **YES (Change)**.

Fails Flip Test, Passes Time-Reversal Test \Rightarrow Temporal.

Example 2 • Source: PerceptionTest • Decision: Temporal

Q: If the person tried to turn on the electric device and it was not working, what was the reason for that?
Options: (A) The electric device did not work most likely because it was already unplugged at the beginning of the video. (B) The electric device did not work because the person unplugged the device during the video. (C) The device worked when the person tried to turn it on.
A: A.

Reasoning.

1. *Horizontal Flip Test*. The question asks about the reason an electric device did not work, specifically whether it was unplugged at the beginning or during the video. Flipping horizontally does not affect the state of the device or the actions performed on it. **NO (No Change)**.
2. *Time-Reversal Test*. The question relies on the chronological order of events — distinguishing the state of the device “at the beginning of the video” versus an action occurring “during the video.” Under reversal, the beginning becomes the end, and an action like “unplugging” would look like “plugging in,” which would alter the correct answer. **YES (Change)**.

Fails Flip Test, Passes Time-Reversal Test \Rightarrow Temporal.

Example 3 • Source: STAR • Decision: Temporal

Q: What did the person do while they were touching the refrigerator?
Options: (A) Closed the refrigerator. (B) Opened the refrigerator. (C) Threw the refrigerator. (D) Took the refrigerator.
A: A.

Reasoning.

1. *Horizontal Flip Test*. If the video is mirrored horizontally, the action of closing the refrigerator remains the same; it does not depend on left/right orientation. **NO (No Change)**.
2. *Time-Reversal Test*. If the video is played in reverse, the action of closing the refrigerator would appear as opening the refrigerator. The answer would change from “Closed” to “Opened.” **YES (Change)**.

Fails Flip Test, Passes Time-Reversal Test \Rightarrow Temporal.

Example 4 • Source: PerceptionTest • Decision: Spatial

Q: In which hand does the person conceal a small object or a drawn sign?

Options: (A) right. (B) I don't know. (C) left.

A: A.

Reasoning.

1. *Horizontal Flip Test.* If the video is mirrored horizontally, the person's right hand will appear as their left hand. The answer to "In which hand..." would change from "right" to "left." **YES (Change).**
2. *Time-Reversal Test.* If the video is played in reverse, the hand in which the object is concealed remains the same hand. The flow of time does not change the identity of the hand holding the object. **NO (No Change).**

Passes Flip Test, Fails Time-Reversal Test \Rightarrow **Spatial.**

Example 5 • Source: PerceptionTest • Decision: Spatiotemporal

Q: The person uses multiple similar objects to play an occlusion game. Where is the hidden object at the beginning of the game from the person's point of view?

Options: (A) Under the first object from the left. (B) Under the second object from the left. (C) Under the third object from the left.

A: B.

Reasoning.

1. *Horizontal Flip Test.* The options explicitly rely on left/right spatial orientation ("first object from the left," "second object from the left"). If the video is mirrored horizontally, the left-to-right order of the objects is reversed, changing the correct answer. **YES (Change).**
2. *Time-Reversal Test.* The question specifically asks about the location of the hidden object *at the beginning of the game*. If the video is played in reverse, the original end of the game becomes the new beginning. Since the object is moved around during the occlusion game, its location at the end is generally different from its location at the start, so the answer changes. **YES (Change).**

Passes both tests \Rightarrow **Spatiotemporal.**

Example 6 • Source: PerceptionTest • Decision: Static

Q: Where is the person?

Options: (A) Indoors in the kitchen. (B) Indoors in the living room or bedroom. (C) Indoors in the bathroom.

A: B.

Reasoning.

1. *Horizontal Flip Test.* If the video is mirrored horizontally (left becomes right), the type of room the person is in (kitchen, living room/bedroom, bathroom) does not change. The answer remains the same. **NO (No Change).**
2. *Time-Reversal Test.* If the video is played in reverse, the setting or room where the person is located does not change. The person stays in the same room regardless of the direction of time. **NO (No Change).**

Fails both tests \Rightarrow **Static.**

D Reward Analysis

D.1 The four CRR reward components

Figure 7 visualizes the four reward terms introduced by CRPO. The original branch combines a correctness reward R_{correct} and a cross-branch CRR reward $R_{\text{CRR}}^{\text{orig}}$ that scores the counterfactual rollouts. The counterfactual branch combines a behavioral reward R_{behave} and a cross-branch CRR reward $R_{\text{CRR}}^{\text{aug}}$ that scores the original rollouts. Both branches additionally use the inherited format reward.

A natural observation from Figure 7 is that the two cross-branch curves $R_{\text{CRR}}^{\text{orig}}$ and $R_{\text{CRR}}^{\text{aug}}$ track each other almost perfectly throughout training. This is not a plotting artifact but a direct consequence

of the symmetric mutual-reward design. Let p denote the fraction of correct rollouts in the original branch and q the fraction of behavior-matching rollouts in the counterfactual branch. By construction, $R_{\text{CRR}}^{\text{orig}}$ activates only on the pG correct original rollouts and each of them measures how often the counterfactual rollouts behave as expected, giving a batch-level expectation of $\lambda \cdot p \cdot q$. The counterfactual side is analogous: $R_{\text{CRR}}^{\text{aug}}$ activates only on the qG behavior-matching counterfactual rollouts and each measures the original branch’s correctness rate p , again yielding $\lambda \cdot p \cdot q$. The two CRR streams therefore receive signals of equal magnitude and neither branch’s reward dominates the other.

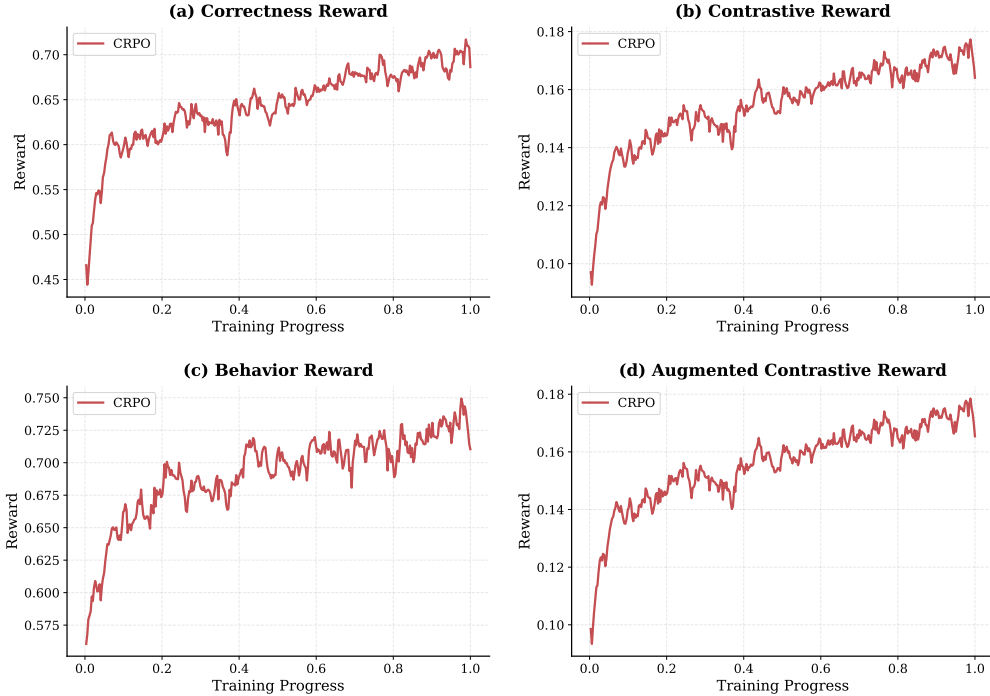


Figure 7: The four reward components introduced by CRPO.

D.2 Training dynamics on Qwen3-VL-8B

Figure 8 plots the same three training-curve diagnostics as Figure 5 in the main paper, but for the larger Qwen3-VL-8B backbone. The trends mirror those observed at 4B. (a) CRPO’s correctness reward again rises more slowly early in training because the CRR penalizes shortcut-based success, but converges to a comparable level by the end. (b) The fraction of zero-advantage groups remains consistently lower for CRPO, confirming that the dual-branch reward provides richer learning signal even at larger scale. (c) The auxiliary temporal rewards of T-GRPO and ArrowRL remain flat, while CRPO’s CRR reward grows steadily, indicating that the 8B model also actively learns to satisfy the counterfactual relation rather than treating it as a side cost. Overall, the similarity between the 4B and 8B dynamics suggests that CRPO’s training behavior is stable across model scales and does not require backbone-specific hyperparameter tuning.

D.3 Sensitivity to reward weights

To probe how robust CRPO is to its two reward coefficients, we run two one-dimensional sweeps on Qwen3-VL-4B and report two complementary metrics, the strict paired metric **DyBench P-Acc** (which most directly reflects spatiotemporal sensitivity) and the standard accuracy **VideoMME** (which reflects general video understanding).

- **Sweep A.** Vary the cross-branch CRR weight $\lambda = \lambda_d = \lambda_s$ over $\{0.0, 0.1, 0.3, 0.5\}$ with $w_{\text{aug}} = 0.5$ fixed. The point $\lambda = 0$ corresponds to a dual-branch GRPO without any CRR signal, isolating the contribution of the relational reward.

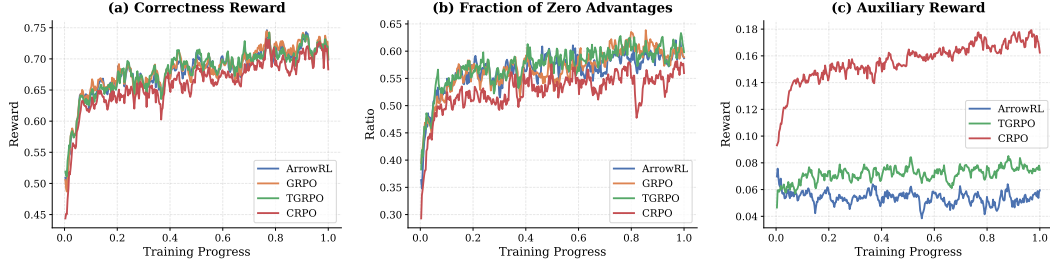


Figure 8: **Training dynamics of CRPO vs. RL baselines on Qwen3-VL-8B.** Same layout as Figure 5 (4B). The trends are consistent across model scales.

- **Sweep B.** Vary the counterfactual-branch weight w_{aug} over $\{0.0, 0.3, 0.5, 0.7\}$ with $\lambda=0.3$ fixed. The point $w_{\text{aug}}=0$ disables policy updates from the counterfactual branch entirely, leaving only the original branch to optimize, while CRR is still computed for diagnostic purposes.

Figure 9 plots the results.

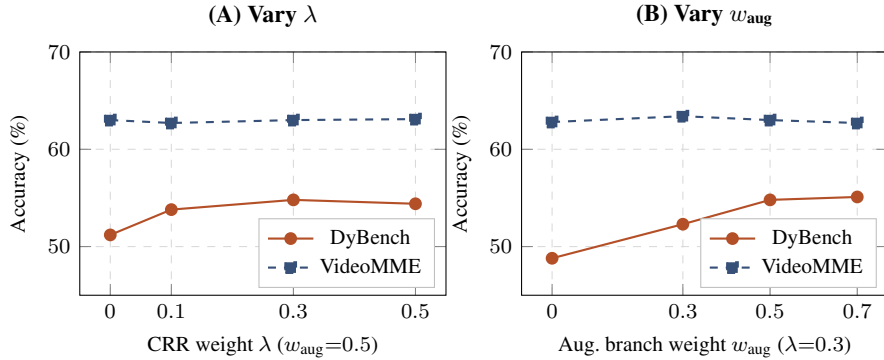


Figure 9: **Sensitivity of CRPO to its two reward coefficients** on Qwen3-VL-4B. Solid orange: DyBench P-Acc (spatiotemporal-sensitive); dashed navy: VideoMME (general). *Left*: varying the cross-branch CRR weight λ with $w_{\text{aug}}=0.5$ fixed. *Right*: varying the counterfactual-branch weight w_{aug} with $\lambda=0.3$ fixed.

Takeaways. (i) Disabling the CRR signal entirely ($\lambda=0$) loses 3.6 points of DyBench P-Acc ($54.8 \rightarrow 51.2$), confirming that the cross-branch relational reward is the main source of CRPO’s gain on spatiotemporal-sensitive evaluation. (ii) Disabling the counterfactual-branch gradient ($w_{\text{aug}}=0$) is even more harmful, costing 6.0 points of DyBench P-Acc ($54.8 \rightarrow 48.8$) and showing that observing counterfactual rollouts without optimizing on them is insufficient. (iii) VideoMME varies by at most 0.7 points across the entire sweep, so CRPO’s reward design does not distort general video understanding regardless of how its two coefficients are set. (iv) Within the interior of each sweep (excluding the zero endpoints), DyBench P-Acc varies by no more than 2.8 points, so CRPO is not sensitive to the precise value of either coefficient as long as both are non-zero.

E CRPO Is Not Standard Data Augmentation

A natural question is whether CRPO’s gain could simply be replicated by standard data augmentation, namely by appending each video’s horizontally flipped or temporally reversed copy to the training set as an extra independent sample with the original label. We argue that the two are fundamentally different in three ways.

Different supervisory targets. Standard data augmentation pretends that the augmented video has the same label as the original. For dynamic questions this is incorrect by construction, since the

answer to a left/right or order question genuinely changes after a flip or reversal. Training a policy on (augmented video, original label) pairs would actively encourage the model to be *insensitive* to dynamics, which is the opposite of what we want. CRPO instead exploits the fact that the answer should change, and uses that expected change as the reward signal.

Cross-branch reward versus per-sample reward. Data augmentation produces independent training samples, each scored only against its own (assumed) label. CRPO computes a reward that depends on the *relation* between answers given to the original and the counterfactual video, namely equivariance for spatiotemporal questions and invariance for static ones. This relational signal cannot be expressed by any per-sample augmentation pipeline, because no single sample carries information about the other branch’s behavior.

No need for counterfactual labels. Standard data augmentation requires either preserving the original label (incorrect for dynamic questions) or producing a new label for the augmented sample (which would require a separate annotation effort). CRPO requires neither counterfactual labels nor process-level evidence annotations, since the cross-branch reward only checks whether the two branches’ answers exhibit the expected relation.

Why the equivariance reward does not lead to reward hacking. A potential concern is that the equivariance term $R_{\text{behave}} = \mathbb{I}[o_j^T \neq o^*]$ only requires the counterfactual answer to be *different* from the original ground truth, not to be the *correct* counterfactual answer. One might worry that the model could learn to produce random outputs on the counterfactual branch to collect this reward. In practice, three properties of CRPO make this strategy difficult to sustain. **First**, both branches share a single policy π_θ , and the original video and its transformation share highly similar visual features (same objects, scene, and motion magnitude). A policy that produces random outputs on the transformed video will degrade on visually similar original videos as well, reducing R_{correct} and thereby the overall reward. A more reliable high-reward strategy is therefore to respond to task-relevant spatiotemporal changes rather than randomize on transformed videos. **Second**, $R_{\text{CRR}}^{\text{orig}}$ activates only when the original branch is correct ($R_{\text{correct}} > 0$), creating a self-regulating feedback loop: any degradation in original-branch accuracy automatically shuts off the CRR signal, so the policy cannot sustain a high CRR reward while sacrificing correctness. Furthermore, because CRPO normalizes advantages using the standard deviation computed jointly across both branches rather than independently per branch, the CRR reward creates a genuine advantage difference that survives normalization and directly influences the policy gradient. **Third**, for static questions (20% of the training set), the reward requires the counterfactual answer to *agree* with the original ($R_{\text{behave}} = \mathbb{I}[o_j^T = o^*]$), which anchors the policy to produce consistent, correct outputs on transformed inputs and discourages a general “randomize on transformed videos” strategy.

F Advantage Normalization and Auxiliary Reward Cancellation

F.1 The cancellation problem in single-branch auxiliary rewards

Standard GRPO computes per-rollout advantages by subtracting the group mean and dividing by the group standard deviation within each prompt’s G rollouts. Recent work has identified that this per-group normalization can be problematic: REINFORCE++ [15] proves that the estimator is biased for small G and proposes global batch-level normalization, while LitePPO [30] shows that using group-level mean with batch-level standard deviation yields more stable training by preventing gradient explosion when within-group reward variance is low.

We observe that this normalization scheme creates a more subtle problem for methods that add auxiliary rewards as constant offsets to correct rollouts. Both T-GRPO [9] and ArrowRL [45] construct a perturbed video (shuffled or reversed) and use it to compute an auxiliary temporal reward that is added to each correct rollout in the original branch. Because the auxiliary reward takes the same value C for all correct rollouts within a group (it depends on group-level statistics, not on individual rollout content), the reward vector after adding C becomes a scaled version of the original reward vector. Formally, let p denote the number of correct rollouts in a group of G . Before the auxiliary reward, correct rollouts receive reward 1 and incorrect rollouts receive 0. After adding the auxiliary reward C to all correct rollouts, the rewards become $1+C$ and 0. The group mean scales from p/G to $p(1+C)/G$, and the group standard deviation scales from σ to $(1+C)\sigma$. After

normalization, the factor $(1+C)$ appears in both numerator and denominator and cancels exactly:

$$\hat{A}_i = \frac{(1+C) - p(1+C)/G}{(1+C)\sigma + \epsilon} \approx \frac{1 - p/G}{\sigma + \epsilon'}, \quad (7)$$

which is the same advantage the rollout would have received without the auxiliary reward. The auxiliary reward therefore has no effect on the policy gradient under per-group mean-std normalization.

F.2 Why CRPO avoids this problem

CRPO’s architecture provides two mechanisms that prevent the cancellation.

Genuine within-group variance from R_{behave} . Unlike T-GRPO and ArrowRL, whose auxiliary reward is a per-group constant, CRPO’s counterfactual branch generates G independent rollouts on the transformed video. The behavioral reward R_{behave} takes different values across these rollouts (some change their answer, some do not), creating genuine within-group variance that survives any normalization scheme. This is the primary learning signal of CRPO and is unaffected by the cancellation problem.

Cross-branch standard deviation. For the CRR terms, which do take a constant value across activated rollouts within a single branch, CRPO computes the standard deviation jointly across both branches’ centered rewards ($2G$ values per prompt) rather than independently per branch. Because the two branches have different reward distributions (the original branch uses R_{correct} while the counterfactual branch uses R_{behave}), the joint standard deviation is not proportional to either branch’s reward scale alone. The CRR constant therefore does not cancel during normalization. This design is motivated by the same insight behind the group-level-mean, batch-level-std normalization advocated by LitePPO [30] and REINFORCE++ [15]: the mean should reflect intra-group ranking while the standard deviation should be computed over a larger pool to prevent constant-factor cancellation and gradient instability.

G Additional Qualitative Examples

Figures 10–15 show additional qualitative comparisons between Qwen3-VL (baseline) and CRPO. The first four examples (Figures 10–13) are drawn from **DyBench**, while the last two (Figures 14–15) are drawn from **TimeBlind** [21]. Across all six pairs, CRPO produces consistent and correct answers on both sides of each counterfactual pair, while the baseline either gives identical answers to both sides (failing the pair) or hallucinates a direction or order that does not match the visual dynamics.

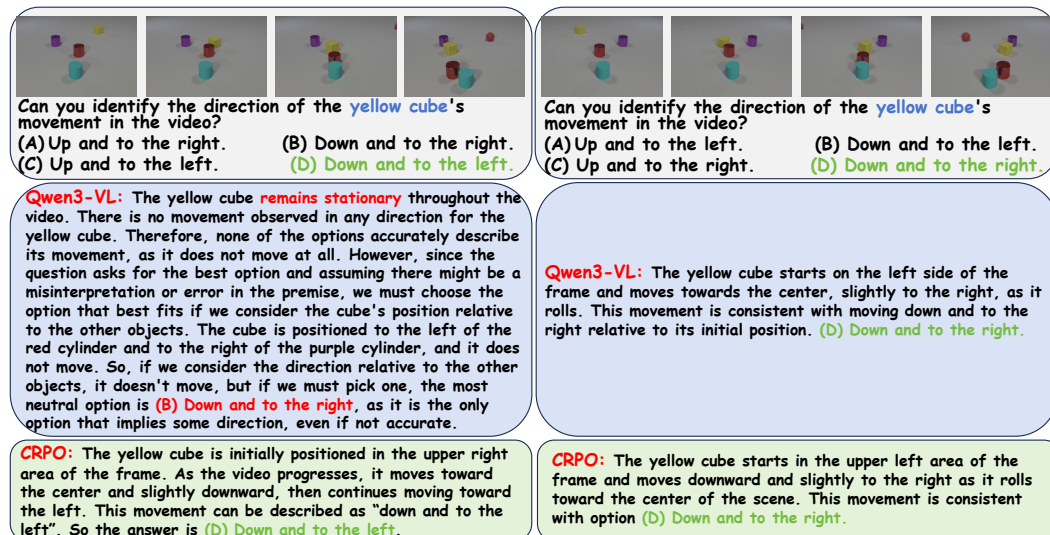


Figure 10: Qualitative example from DyBench (*moving direction*): identifying which way the yellow cube moves on opposite paired videos.

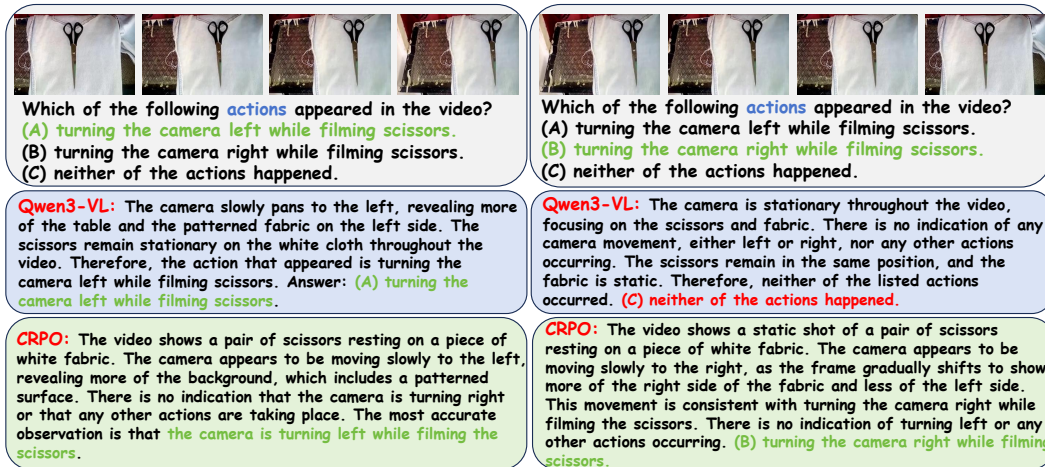


Figure 11: Qualitative example from DyBench (*moving direction*): identifying whether the camera pans left or right while filming the scissors.

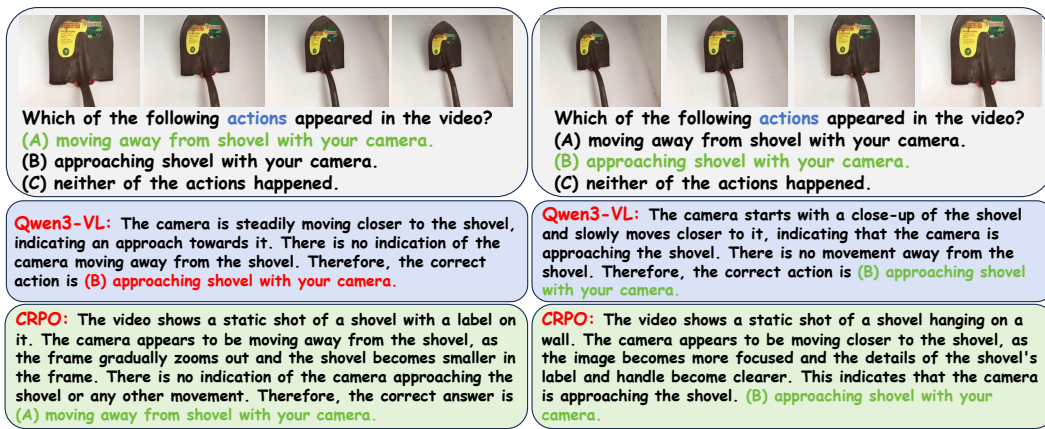


Figure 12: Qualitative example from DyBench (*moving direction*): identifying whether the camera is approaching or moving away from the shovel.

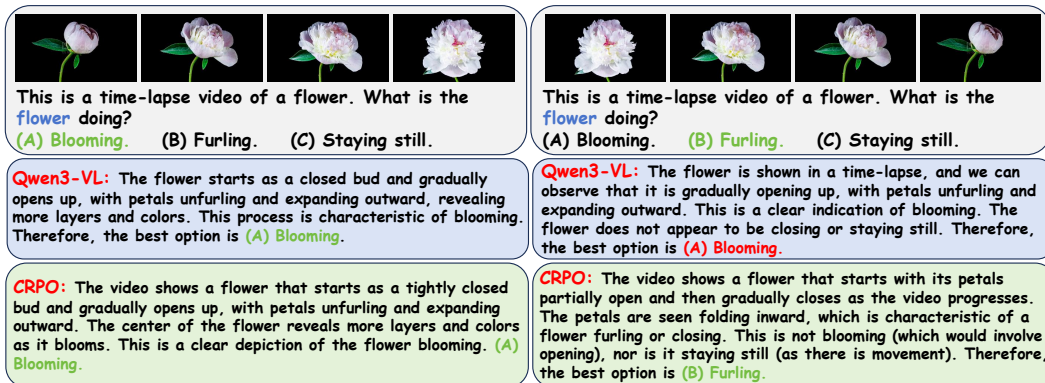
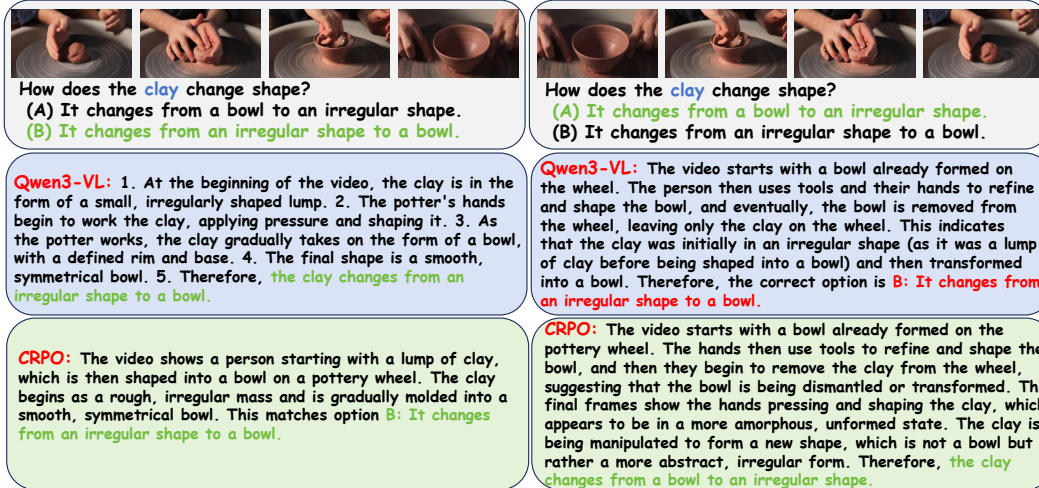


Figure 13: Qualitative example from DyBench (*reversible dynamics*): identifying whether a time-lapse of a flower shows blooming or furling.



How does the clay change shape?
 (A) It changes from a bowl to an irregular shape.
 (B) It changes from an irregular shape to a bowl.

Qwen3-VL: 1. At the beginning of the video, the clay is in the form of a small, irregularly shaped lump. 2. The potter's hands begin to work the clay, applying pressure and shaping it. 3. As the potter works, the clay gradually takes on the form of a bowl, with a defined rim and base. 4. The final shape is a smooth, symmetrical bowl. 5. Therefore, the clay changes from an irregular shape to a bowl.

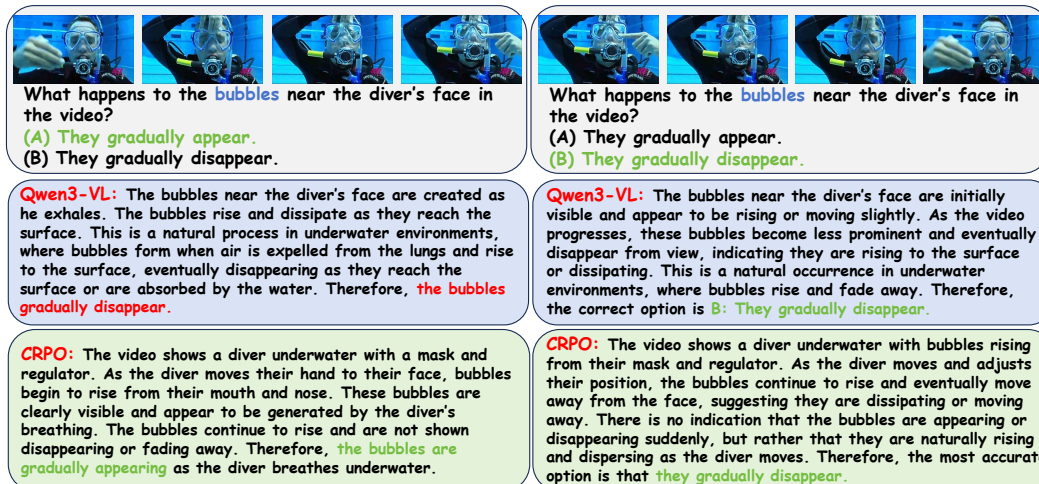
CRPO: The video shows a person starting with a lump of clay, which is then shaped into a bowl on a pottery wheel. The clay begins as a rough, irregular mass and is gradually molded into a smooth, symmetrical bowl. This matches option B: It changes from an irregular shape to a bowl.

How does the clay change shape?
 (A) It changes from a bowl to an irregular shape.
 (B) It changes from an irregular shape to a bowl.

Qwen3-VL: The video starts with a bowl already formed on the wheel. The person then uses tools and their hands to refine and shape the bowl, and eventually, the bowl is removed from the wheel, leaving only the clay on the wheel. This indicates that the clay was initially in an irregular shape (as it was a lump of clay before being shaped into a bowl) and then transformed into a bowl. Therefore, the correct option is B: It changes from an irregular shape to a bowl.

CRPO: The video starts with a bowl already formed on the pottery wheel. The hands then use tools to refine and shape the bowl, and then they begin to remove the clay from the wheel, suggesting that the bowl is being dismantled or transformed. The final frames show the hands pressing and shaping the clay, which appears to be in a more amorphous, unformed state. The clay is being manipulated to form a new shape, which is not a bowl but rather a more abstract, irregular form. Therefore, the clay changes from a bowl to an irregular shape.

Figure 14: Qualitative example from TimeBlind: identifying whether the clay changes from a lump to a bowl, or from a bowl to a lump.



What happens to the bubbles near the diver's face in the video?
 (A) They gradually appear.
 (B) They gradually disappear.

Qwen3-VL: The bubbles near the diver's face are created as he exhales. The bubbles rise and dissipate as they reach the surface. This is a natural process in underwater environments, where bubbles form when air is expelled from the lungs and rise to the surface, eventually disappearing as they reach the surface or are absorbed by the water. Therefore, the bubbles gradually disappear.

CRPO: The video shows a diver underwater with a mask and regulator. As the diver moves their hand to their face, bubbles begin to rise from their mouth and nose. These bubbles are clearly visible and appear to be generated by the diver's breathing. The bubbles continue to rise and are not shown disappearing or fading away. Therefore, the bubbles are gradually appearing as the diver breathes underwater.

What happens to the bubbles near the diver's face in the video?
 (A) They gradually appear.
 (B) They gradually disappear.

Qwen3-VL: The bubbles near the diver's face are initially visible and appear to be rising or moving slightly. As the video progresses, these bubbles become less prominent and eventually disappear from view, indicating they are rising to the surface or dissipating. This is a natural occurrence in underwater environments, where bubbles rise and fade away. Therefore, the correct option is B: They gradually disappear.

CRPO: The video shows a diver underwater with bubbles rising from their mask and regulator. As the diver moves and adjusts their position, the bubbles continue to rise and eventually move away from the face, suggesting they are dissipating or moving away. There is no indication that the bubbles are appearing or disappearing suddenly, but rather that they are naturally rising and dispersing as the diver moves. Therefore, the most accurate option is that they gradually disappear.

Figure 15: Qualitative example from TimeBlind: identifying whether the bubbles near the diver's face gradually appear or gradually disappear.

H Limitations and Broader Impact

Limitations. CRPO requires the construction of a counterfactual visual input for each training prompt, and we currently restrict the transformations to spatial flips and temporal reversals, both of which can be applied to arbitrary videos. Extending CRPO to more semantically rich counterfactual transformations (e.g., object substitution, scene relighting) would require either generative video editing or a curated counterfactual data source, and is left for future work. The Task Router is run offline by a separate reasoning model and incurs an additional one-time pre-processing cost. Finally, DyBench focuses on short videos (median length under 10s) and does not yet stress-test long-horizon temporal reasoning.

Broader impact. By directly penalizing shortcut-based policies during RL post-training, CRPO produces Video LLMs whose answers are more faithfully tied to the actual spatiotemporal content of the video. We expect this to make Video LLMs more reliable in downstream applications such as instructional video assistance and accessibility tools, where misreading the direction or order of

an event can cause real harm. We do not foresee additional negative societal impacts beyond those already discussed in the literature on Video LLMs.